Role Of MRI in of painful wrist joint

(Essay)

Submitted for partial fulfillment of
master degree in radiodiagnosis.

By

Ahmed Saad El-Din Ali maaly
M.B.B.CH

Under supervison of

Prof. Dr.
Mostafa Sonbol
Prof. Of Radiodiagnosis
faculty of medicine
Al-Azhar university

Prof. Dr.
Ismail A. Hammuda
Prof. of Orthopedic
faculty of medicine
Al-Azhar university

Prof. Dr.
Hussein Abd Elaziz
Assist. Prof. of Radiodiagnosis
faculty of medicine
Al-Azhar university

Al-Azhar university
faculty of medicine 2006

بِسْمِ اللَّهِ الرَّحْمَٰنِ الرَّحِيمِ

﴿ قَالُوا سُبْحَانَكَ لَا عِلْمَ لَنَا إِلَّا مَا عَلَّمْتَنَا ۖ

إِنَّكَ أَنتَ الْعَلِيمُ الْحَكِيمُ ﴾

صدق الله العظيم

سورة البقرة (آية 32)

Acknowledgement

First and foremost, thanks to Allah who gave me the ability to complete this work

I would like to express my sincere and deep gratitude to my **prof. DR. Mostafa F. Sonbol** .prof. of radiodiagnosis, faculty of medicine, Al-Azhar University for his kind help, cooperation, and encouragement. it is a great honor to work under his guidance and supervision.

Also I am very grateful to **prof. DR. Ismail A. Hamoda** prof. Of orthopedic ,faculty of medicine, Al-Azhar univeristy and **prof. DR. Hussein Abd Elaziz** .prof. of radiodiagnosis, faculty of medicine, Al-Azhar University .for ther valuable help and been interest in the progress and accomplishment of this work.

Content

Title	Page
Introduction & Aim of the work	1
Osseous anatomy	3
Joint compartment of the wrist	9
Ligaments	12
Triangular fibrocartilage complex	17
Carpal tunnel	18
Tendons	20
MRI anatomy of the wrist	22
Technique & protocol	30
Nerve intrapment syndrome	35
Ligamentous lesion.	44
Triangular fibrocartilage abnormalities	49
Tendon abnormalities	59
Avascular bone necrosis	63
Synovial lesions	74
Masses of the wrist	77
Summary	87
Conclusion	89
References	90
Arabic summary	97

List of figures

Figure	Title	page
1	Osseous structures of the hand and wrist	1
2	Gradient echo coronal images demonestrating the scaphoid	2
3	(A): Coronal gradient echo image demonstrating the lunate (B): Sagittal T1_WI demonestrating the lunate .	3
4	Coronal T1_weithed image demonstrating a type 2 lunate	4
5	(A):Coronal gradient echo image demonstrates triquetrum (B): Axial T1_WI demonestrates triquetrum .	4
6	Coronal T1_weithed image demonstrates hamate	6
7	Axial image at distal Radioulnar joint	7
8	indirect MR arthrogram demonestrates TFCC	8
9	Midcarpal joint	9
10	palmar carpal ligaments	10
11	Coronal image of radioscaphocapitate ligament	11
12	Coronal image of palmar radiocarpal ligaments	12
13	Dorsal carpal ligaments	12
14	Sagittal T1 of ulnocarpal ligaments	14
15	Coronal T1 of palmar midcarpal ligaments	15
16	Fat-suppressed T2 of normal TFCC	15
17	Axial image demonestrates carpal tunnel	17
18	Coronal T1 demonestrates flexor tendons	18
19	Axial T2 demonestrates extensor tendons	19
20	Axial T2 at level of distal forearm	21
21	Axial T2 at level of carpal bone	22
22	Axial T2 at level of carpal bone	22
23	Sagittal T1 of normal wrist	24
24	Sagittal gradient image of normal wrist	25
25	Coronal T2-weighted of the wrist	27
26	Coronal T2-weighted of the wrist	27
27	Coils for hand and wrist	30
28	Axial image at level of hook of hamate show median nerve	34
29	Axial T2*-WI(A)swelling of median nerve(B)high signal nerve	35
30	Axial T2-W gradient images show different stages of CTS	37
31	Axial T1-WI show lipomatosis of median nerve	38
32	Incomplete release of the flexor retinaculum	39
33	Neurofibroma of median nerve	39
34	Guyon tunnel syndrome	41
35	Axial T1 show scapholunate ligament tear	43
36	Coronal image of normal variance of scapholunate ligament	44
37	(A)Coronal MR arthrogram, (B)Coronal unenhanced, images show abnormal high signal of lunotriquetral ligament	45
38	Class IA (traumatic) TFCC	47
39	Class IB (traumatic) TFCC	48
40	Class IC (traumatic) TFCC	48
41	Class ID (traumatic) TFCC	49

Figure	Title	page
42	Class IIA (degenerative) TFCC	50
43	Class IIB (degenerative) TFCC	50
44	Class IIC (degenerative) TFCC	51
45	Class IID (degenerative) TFCC	51
46	Class IIE (degenerative) TFCC	52
47	Pathology of ulnar impaction syndrome	53
48	Coronal **(A)** TI-WI, **(B)** Gradient-echo, images show ulnar impaction syndrome	54
49	Coronal gradient image show ulnar impaction syndrome	55
50	Axial T1 show distal radioulnar joint impaction	56
51	T1-weighted sagittal image show Complete disruption of the flexor digitorum superficialis and profundus tendons	58
52	De Quervian's tenosynovitis	59
53	Tenosynovitis of the extensor carpi-ulnaris tendon	60
54	Coronal images show fracture of distal radius	61
55	Coronal image show scaphoid fracture	62
56	Preiser's disease	63
57	Coronal**(A)**T1**(B)**T2,images show avascular necrosis of scaphoid	64
58	Avascular necrosis of proximal pole of scaphoid	64
59	AP radiograph shows diffuse sclerosis of the scaphoid.	65
60	Coronal images shows diffuse sclerosis of the scaphoid while fracture line is not identified	65
61	AP radiograph displays sclerosis and collapse of the lunate	67
62	Stage I Kienböck's disease	68
63	Stage II Kienböck's disease	68
64	Stage III Kienböck's disease	69
65	Axial CT scan demonstrating fracture of the hook of the hamate	70
66	Positive ulnar variance	70
67	Negative ulnar variance	71
68	Pigmented villo nodular synovitis	72
69	Coronal **(A)** T1 **(B)** T2* images show synovial cyst	74
70	Enchondroma	76
71	Giant cell tumor	78
72	Osteoid osteoma	79
73	Aneurysmal bone cyst	80
74	A large ganglion cyst	82
75	Lipoma	83

List of abbreviations

APB	:adductor pollicis brevis.
APL	: adductor pollicis longus.
AVN	:avascular bone necrosis.
CTS	:carpal tunnel syndrome.
DRUJ	:distal radioulnar joint.
EUC	:extensor carpi-ulnaris.
FS	:fat suppression.
FSE	:fast spin echo
Gd	:gadolinium.
GRE	:gradient.
KD	:kienbock's disease.
L	:lunate.
LRL	:long radiolunate.
LT	:lunotriquetrum.
MRI	:magnetic resonance imaging.
PVNS	:pigmented villonodullar synovitis.
R	:radius.
RA	:rheumatoid arthritis.
RLT	:radiolunotirquetrum.
ROI	:region of interest
RSC	:radioscaphocapitate.
RSL	:radioscapholunate.
S	:scaphoid.
SL	:scapholunate.
SNR	:signal to noise ratio.
STIR	:short time inversion recovery.
T	:triquetrum.
T1	:relaxation time1.
T2	: relaxation time2.
TE	:echo time .
TFCC	:triangular fibrocartilage complex.
TR	:time of repetition
U	:ulna.
V	:volar.
WI	:weighted image.

Introduction & Aim of the Work

Introduction

Magnetic resonance imaging provides visualization of the complex anatomy of the wrist and delineation of numerous pathologic processes, which are difficult to visualize with conventional imaging modalities(**Siegel et al .,1996).**

MR imaging allows earlier detection of an abnormality in the triangular fibrocartilage complex or bone marrow of carpal bones and is helpful in formulating the extensive differential diagnosis in patients with ulnar wrist pain and limitation of motion **(cerezal et al., 2002).**

High resolution Magnetic resonance imaging permits accurate detection and localization of tears of the TFCC. Magnetic resonance imaging is an accurate and effective method for non invasive evaluation of pain in the wrist **(potter et al., 1997).**

MR is the investigation of choice in avascular necrosis and has an increasing role in internal derangement, trauma and soft tissue lesion **(Seymour and White, 1998).**

MRI can directly visualize and monitor changes in synovium and bone that precede actual bone necrosis **(peterfy, 2001).**

Aim of the work

To evaluate the diagnostic value of MRI in patient with painful wrist and to detect the underlying causes.

ANATOMY

Osseous anatomy:

There are 8 carpal bones in the wrist, the proximal carpal rows(scaphoid, lunate, triquetrum & pisiform) articulates with distal radius and unla ***(Carcia-Elias and Dobyns, 1998).***

Distal row consist of (from lateral to medial): trapezium, trapezoid, capitate and hamate **(Fig.1).**

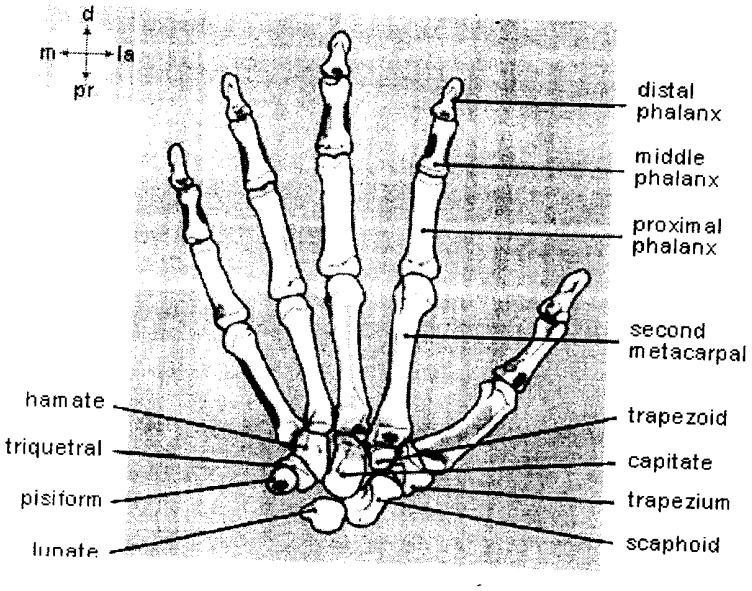

Fig.(1) The bones of the hand., particularly in the carpus, have been slightly separated to reveal their articular surfaces **(Quoted from Stoller and Brody 1997).**

Scaphoid:

It is the largest carpal bone in the proximal row and serves as an important link between the proximal and distal carpal rows ***(Schimmel-Metz, et al., 1999).***

The scaphoid articulates with the radius and lunate medially, the capitale distomedially and trapezium and trapezoid distally **(Fig.2)** ***(Berquist 2003).***

The scaphoid ridge is located on the mid-lateral surface and accept about 80% of the vascular supply of the scaphoid ***(Rosse and Rosse, 1997).***

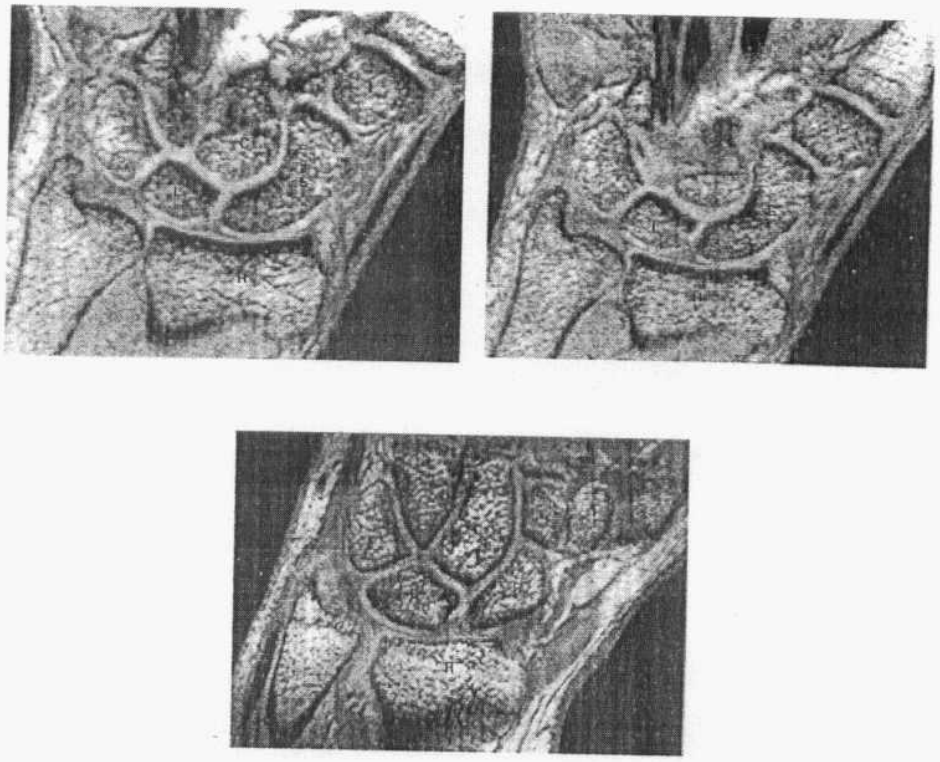

Fig.(2) Gradient echo coronal images demonestrating the scaphoid (S) and its Articulations with the radius ,lunate, capitate and trapezium and trapezoid distally **(Quoted from Berquist,2003).**

Lunate:

The lunate is rectangular in coronal plane. about 80% of the surface is covered by articular cartilage.

The lunate has four articular surfaces for radius proximally, scaphoid laterally, triquetrum medially and capital and hamate distally. There are palmar and dorsal non articualr surface **(Fig.3).**

(A) **(B)**

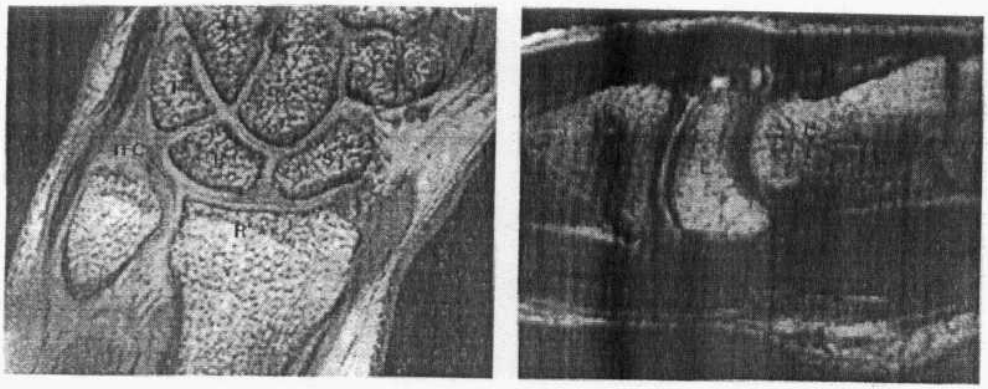

Fig.(3) (A): Coronal gradient echo image demonstrating the lunate and its Articulations with triangular fibrocartilage (TFC), radius (R), scaphoid, Triquetrum and capitate. this is type 1 lunate (no hamate articulations.

(B): sagittal T1_weighed MR arthrogram demonstrating the moon _shaped appearance of the lunate and aligned articulations with the radius (R) and and capitate **(Quoted from Berquist 2003).**

Lunate described as 2 types based on the articulation with hamate:

Type I: has no hamate articulation.

Type 2: has hamate articulation facet**(Fig.4)** ***(Carcia-Elias and Dobyns, 1998).***

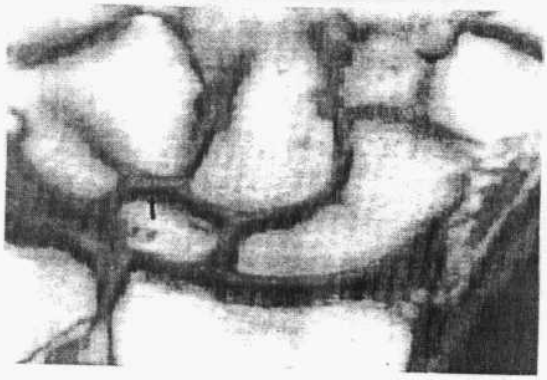

Fig.(4) Coronal T1_weithed image demonstrating a type 2 lunate with a small (arrow) Hamate facet **(Quoted from Berquist, 2003).**

Triquetrum:

Triquetrum has four articualr facets. the proximal surface articulate with ulna & triangular fibrocartilage complex, the distal surface articulates with hamate, radial surface articulates with lunate the distal anterior surface articulates with pisiform, anterior and posterior surfaces are roughened for ligament atteachments **(Fig.5)** ***(Rosse and Rosse, 1997).***

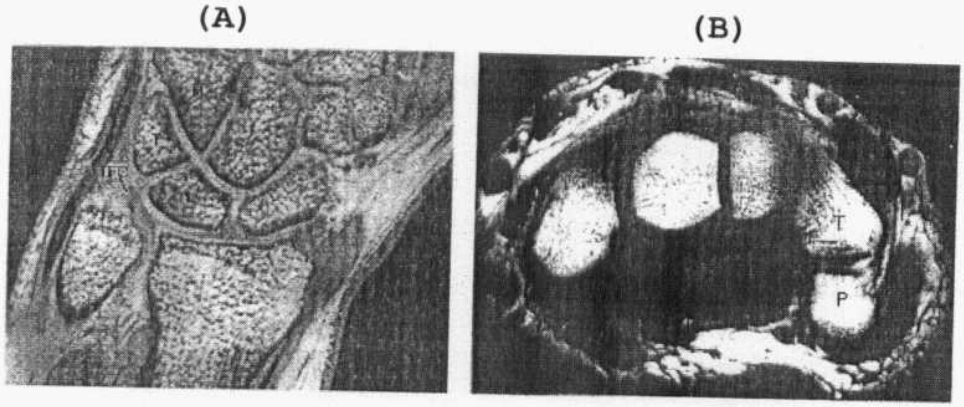

Fig.(5) (A): Coronal gradient echo image demonstrating the articulations of theTriquetrum with trinagular fibrocartilage , lunate , and hamate.**(B):**Axial T1_weithwd image demonstrating articulation of the triquetrum withThe pisiform **(Quoted from Berquist, 2003).**

Pisiform:

Flexor carpiulnaris tendon attaches to the pisiform, it has one facet which articulates with triquetrum ***(Berquist, 2003).***

Trapezium:

The trapezium has four articular surface, the ulnar facet articulates with the trapezoid, proximal facet articulates with scaphoid, distally there is small one for articulation with the base of 2nd metacarpal & large one for articulation with 1st metacarpal.

On the palmar aspect there is groove for the flexor carpi radialis tendon and ridge for attachment of flexor retinaculum, scapho-trapezial and anterior oblique ligaments ***(Carcia –Elias and Dobyns, 1998).***

Trapezoid:

Trapezoid has four articular surfaces, the distal one for articulation with 2nd metacarpal the radial facet for articulation with trapezium, unlar facet for articulation with capitate and proximal facet for articulation with scaphoid ***(Rosse and Rosse, 1997).***

Capitate:

The capitate is the largest carpal bone, the proximal capitate is termed the head of capitate which is covered with articualr cartilage and has 3 facets for articulation with scaphoid, lunate and hamate.

The distal radial aspect is termed the body, it has facets for articulation with trapezoid, 2nd and 3rd metacarpal ***(Rosse and Rosse, 1997).***

In 85% of patients there is small facet for 4th metacarpal base ***(Viegas et al., 1991).***

Hamate:

The hamate has a prominent palmar projection (hook) which form the medial boundary of the carpal tunnel, the tip of the hook give attachment for flexor retinaculum & pisohamatum ligament **(Fig.6)**.

Distally it articulates with 4th & 5th metacarpal bases. proximally and medially it articulates with triquetrum, radial aspect articulates with capitate ***(Rosse and Rosse,1997).***

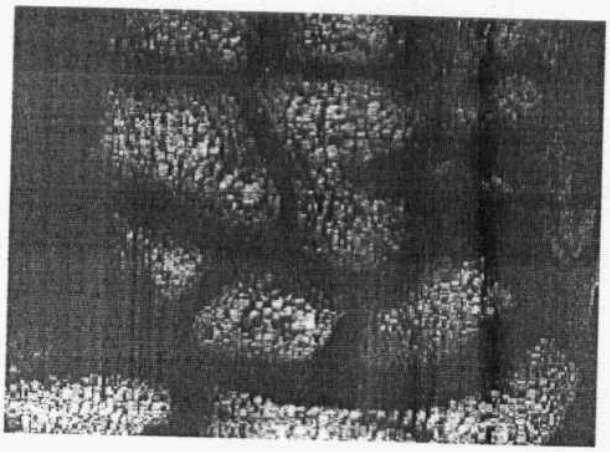

Fig. (6) Coronal T1_weithed image demostrate the radial styloid process, scaphoid, Lunate,capitate,and hamate **(Quoted from Berquist, 2003).**

Joint Compartments of Wrist Joint

Three joint compartments are described:

(A) ***Distal Radioulnar joint*** **(Fig.7):**

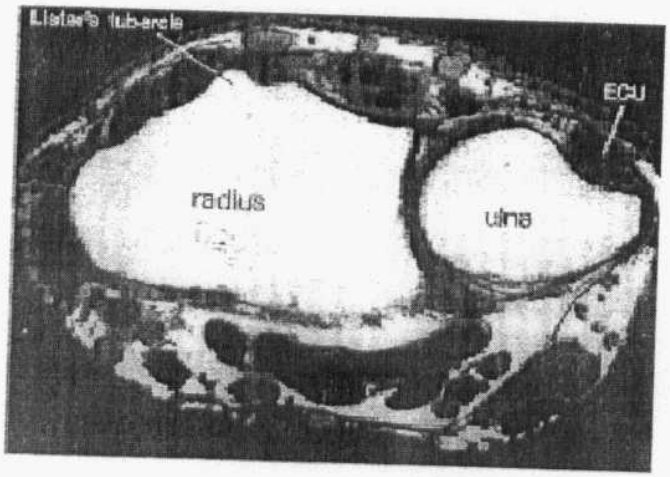

Fig.(7) Axial image at the distal radioulnar joint demonstrating the articulation Of the radius and ulna **(Quoted from Berquist, 2003).**

Distal radioulnar joint is stabilized by TFCC ***(Berquist, 1992).***

TFC connects the ulna and radius at their most distal edges and separate DRUJ from radiocarpal joint. TFC runs from the ulnar edge of the lunate facet to the base of the ulnar styloid, where it inserts into small depression in the distal ulna known as fovea ***(Bogumill, 1988).***

The ulnar portion of the TFCC is vascularized by branches of the ulnar and posterior interosscous arteries, the central and radial aspects are essentially arascular ***(Carcia Elias et al., 1998).***

The central region frequently degenerates after age of 40 resulting in signal abnormalities (increased signal intensity) on MR images ***(Theuman, et al., 2002).***

TFCC consists of : TFC, dorsal and volar radioulnar ligaments, sheath of extensor carpi-ulnaris tendon, ulnocarpal ligaments, ulnar collateral ligament and ulno meniscal homologue (ulnar carpal meniscus) ***(Georges , et al., 2003).***

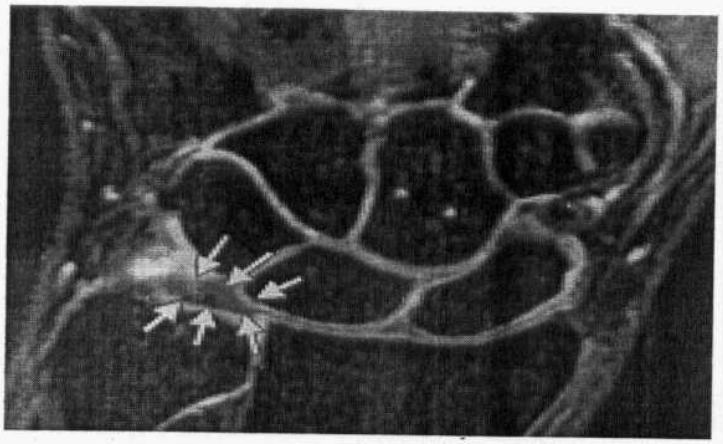

Fig. (8) Coronal three-dimensional gradient-echo indirect MR arthrogram illustrates a normal low-signal-intensity appearance of the central disk of the TFCC (arrows) **(Quoted from Haims, et al ., 2003).**

(B) Radiocarpal joint:

Radiocarpal joint is defined by TFC and the distal radial surface proximally. lunate, triquetrum and scaphoid distally ***(Bogumill, 1998).***

(C) Midcarpal joint:

Covers the spaces between carpal rows Extends into the carpometacarpal articulations ***(Gray, 1987).***

The midcarpal joint is formed between the proximal and distal carpal rows. The midcarpal joint cavity is located primarily between the distal aspects of scaphoid, lunate and triquetrum and proximal aspect of the distal row.

Proximal extension to mid carpal joint (between scaphoid & lunate and lunate & triqueterum) is limited by interosseous ligaments, while distal extension to mid carpal joint are located between the four bones of distal carpal row **(Fig. 9)** ***(Stoller and Brody, 1997).***

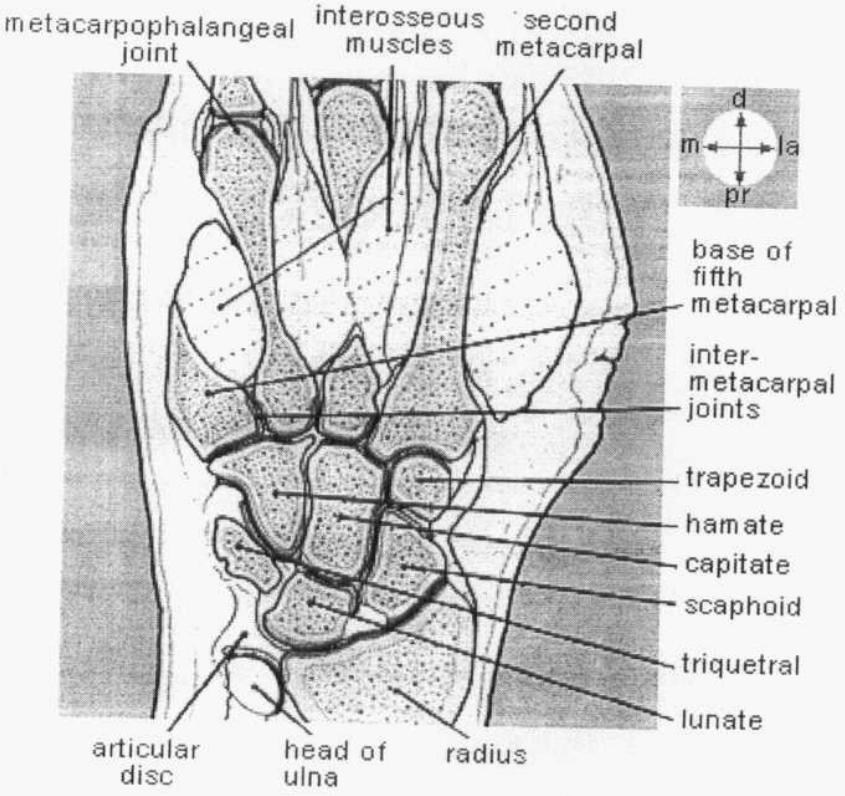

FIG.(9) A coronal section of the hand shows the joints of the carpal region. (**Quoted from Stoller and Brody, 1997**).

Ligamentous anatomy

The ligaments of the wrist are generally divided into extrinsic, binding the radius to the carpals and intrinsic, binding the carpal bones to one other *(Scott et al., 1997).*

A) Palmar ligaments (Fig.10):

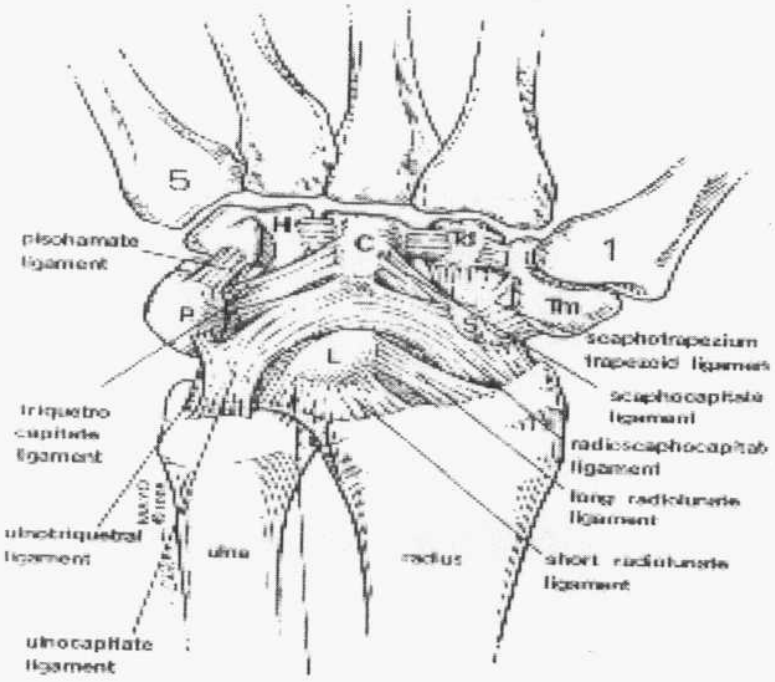

Fig.(10) An illustration of the palmar carpal ligaments **(Quoted from Berquist,2003).**

Radioscaphocapitate ligament is the most lateral of palmar ligaments originate at radial styloid and palmar radial margin and extend to scaphoid ridge then to capitate where it joint the ulnocapitate ligament to form arcuate ligament **(Fig.11)** *(Berger, 1998).*

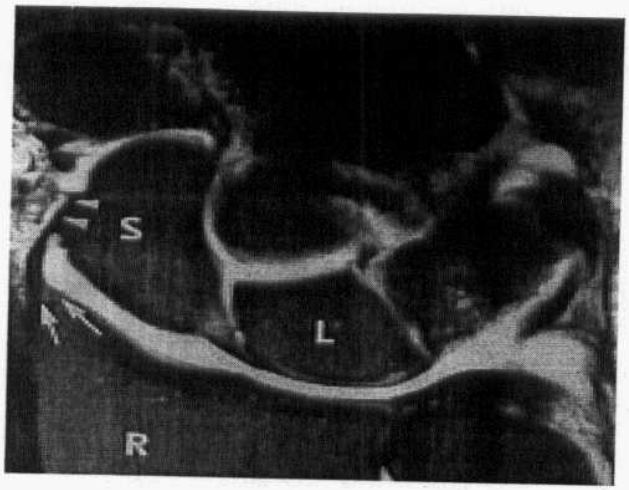

Fig. (11) Coronal T1-weighted fat-saturated spin-echo MR arthrographic image of the wrist. The radial collateral ligament arises from the tip of the radial styloid process (arrows) and extends distally to the lateral aspect of the scaphoid *(S)* waist (arrowheads). *L* = lunate, *R* = radius **(Quoted from Theuman , 2002).**

Long radiolunate ligament : Originates form palmar distal radius medial to radioscaphocapitate ligament, the ligament overlap the radioscaphocapitate ligament to insert on the palmar radial aspect of lunate ***(Berger et al., 1998).***

Radioscapholunate ligament : originates from ulnar aspect of distal radius, and extend between long and short radiolunate ligaments to insert on the lunate and medial scaphoid.

Short radiolunate ligament : originates from palmar medial radius and extend to insert on the palmar surface of lunate**(Fig.12)** ***(Berger, 1998).***

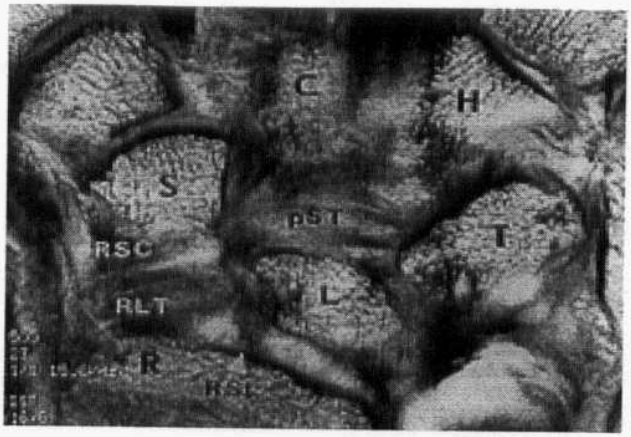

Fig.(12) Coronal T1-weighted spin-echo MR arthrographic image demonestrates Palmar radiocarpal and intercarpal ligaments. the capitate *(C)* , The palmar scaphotriquetral ligament *(pST)*, scaphoid *(S)*, triquetrum *(T)*, radioscapholunate *(RSL)*,. The long radiolunate (RLT) and radioscaphocapitate (RSC) **(Quoted from Theuman 2002).**

B) Dorsal ligament (Fig.13):

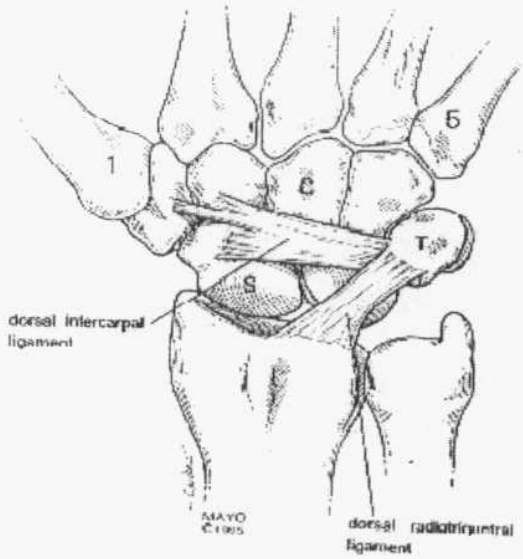

Fig.(13) illustration of the dorsal carpal ligaments **(Quoted from Berquist, 2003).**

Dorsal radiocarpal ligament originates from the distal radius on the ulnar side of lister's tubercle and pass obliquely to insert on the triquetrum (superficial fibers) and lunate (deep fibers).

Dorsal intercarpal ligament originates from triquertrum and extend to insert by 3 slips on the scaphoid, trapezium and trapezoid ***(Brown et al., 1998).***

C) UlnoCarpal ligaments (Fig. 14):

Originate primarily from palmar radioulnar ligament at margin of TFCC.

Ulnolunat ligament : is contiguous with the short radiolunate ligament.

Ulnotriquetral ligament: arise just medial to ulnolunate ligament from palmar radioulnar ligament.

Ulno capitate ligament: originates from the base of ulnar styloid and palmar radioulnar ligament, it takes course palmar to the above ulnocarpal ligaments and insert on the triquetrum, pisiform and pisotriquetral ligament ***(Berger, 1998).***

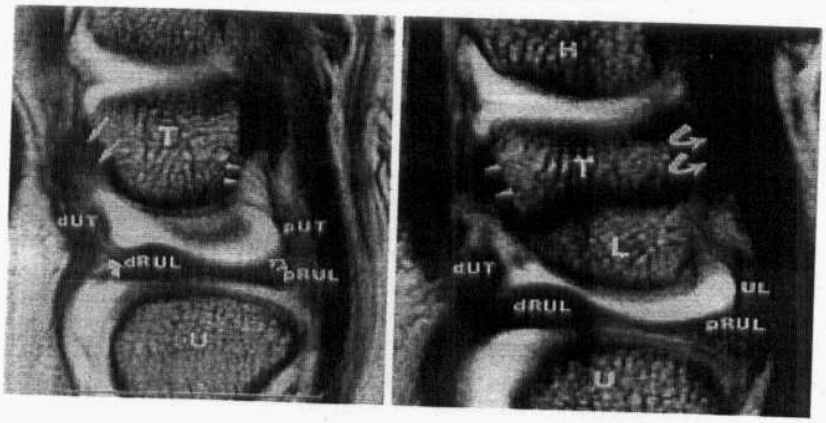

Fig.(14) Sagittal T1-weighted spin-echo MR arthrographic image of the wrist.demonstrate The palmar ulnolunate ligament *(UL)*, dorsal radioulnar ligament (*dRUL*, *palmar* radioulnar ligament *(pRUL)*, lunate *(L)*, *dorsal* ulnotriquetral ligament *(dUT)*, triquetrum *(T)*, palmar ulnotriquetral ligament *(pUT)*, **(Quoted from Theuman, 2002).**

D) Palmar midcarpal ligaments (Fig. 15):

The palmar midcarpal ligaments are contiguous with the radiocarpal and ulnocarpal ligaments as they join to form a nearly contiguous palmar capsule volar to intercarpal joints.

- ***Scaphotriquetral ligament.***
- ***Scapho capitate ligament.***
- ***Triquetro capitate ligament.***
- ***Triquetro hamate ligament.***
- ***Pisohamate ligament.***

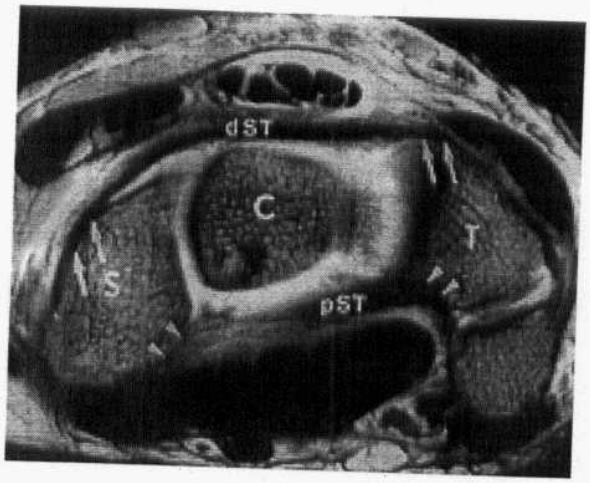

Fig. (15) Coronal T1-weighted spin-echo MR arthrographic image of the wrist demonstrates dorsal scaphotriquetral ligament *(dST) and* palmar scaphotriquetral ligament *(pST)* **((Quoted from Theuman, 2002).**

Triangular fibrocartilage complex (TFCC) (Fig.16):

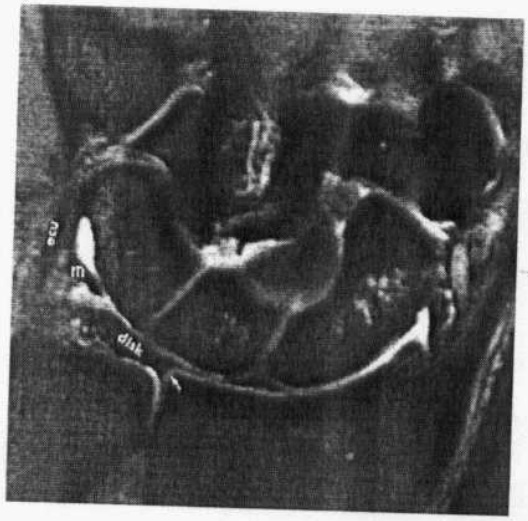

Fig. (16) Fat-suppressed T2-weighted fast spin-echo coronal image of the normal TFCC. The biconcave central disk (disk), extensor carpi ulnaris (ecu), meniscal homologue (m), and cartilage of the radial sigmoid notch (arrow) are identified **(Quoted from stoller and Brody, 1997).**

TFCC consist of triangular fibrocartilage (TFC) dorsal and volar radioulnar ligament, sheath of extensor carpi-ulnaris tendon, ulnocarpal ligaments, ulnar collateral ligament and ulno-meniscal homologe. TFC separates the radio-carpal and inferior radio-ulnar compartements, TFC is thicker peripherally then centrally, and it may show central fenestration, TFCC is an important soft tissue structures that serves as cushion between the carpal bones and distal ulna & radius and contributes to the stability of inferior radioulnar joint ***(Georges , et al., 2003).***

Carpal tunnel:

The carpal tunnel is a fibro-osseous space on the volar aspect of the wrist. The roof is formed by flexor retinaculum which is composed of fibrous bands running between pisiform & the hook of hamate ulnarly, and the tubercles of the scaphoid & trapezium radially, the floor is formed by capitate and lunate, the radial wall is formed by the tubercle of the trapezium and the ulnar wall is formed by the hook of hamate ***(Chein , et al., 2001).***

Through the tunnel course the eight flexor digitorum tendons, tendon of flexor policis long and and median nerve, carpal tunnel is the most common site of peripheral nerve entrapment **(Fig.17)** ***(Scott, et al., 1997).***

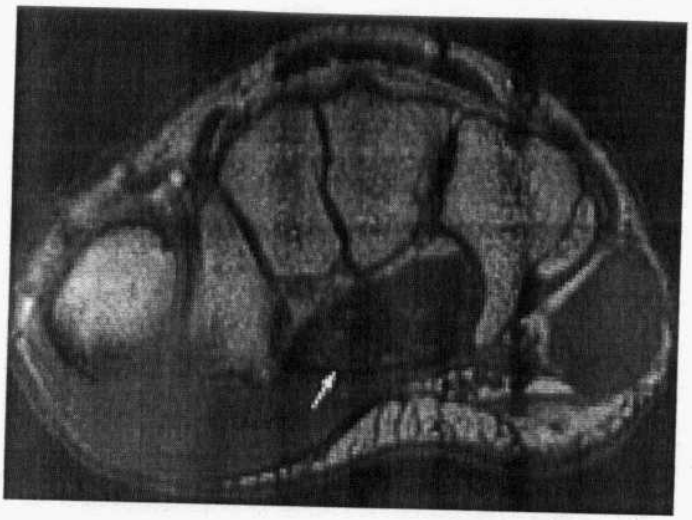

Fig.(17) Transverse T1-weighted at the level of the hook of the hamate demonstrate visibility of the median nerve (arrow)(**Quoted from Nadja Saupe, et al.,2005).**

Guyon's canal:

Guyon's canal begins at the palmar carpal ligament and extends 4-5 cm to the fibrous arch of the hypothenar muscles, it's bounded by volar carpal ligament, transverse carpal ligament and medially by the pisiform and flexor carpi-ulnaris tendon. ***(Sakai , et al., 2000).***

The canal contain ulnar nerver, artery and occasionally ulnar veins and anomalous muscles. Although nerve compression here is far less common than in the carpal tunnel, it's a potential site of ulnar nerve entrapment ***(Scott et al., 1997).***

Tendons

Flexor tendons (FIG.18):

The long flexor tendons of the fingers and thumb are beneath the flexor retinaculum withen the carpal tunnel in the wrist. the four flexor digitorum superficialis tendons are arranged in 2 rows tendons to the ring and middle fingers above tendons to index and little fingers. The four flexor digitorum profundus tendons are deep to the superficialis ***(Mesgarzadeh et al., 1996).***

Flexor carpi-radials tendon pass a long the radial aspect of the carpal tunnel and separated from the other tendons by deep lamina of flexor retinaculum.

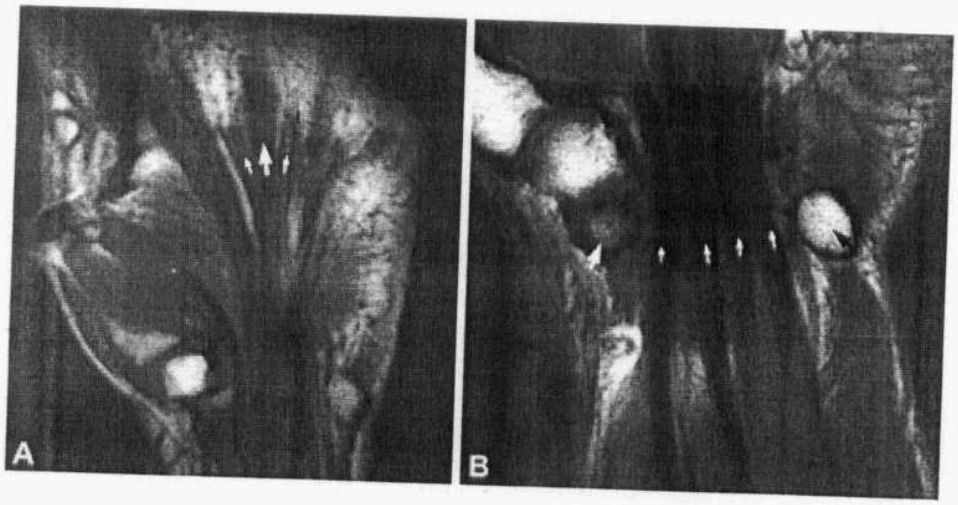

FIG.(18):(A) T1_W coronal image shows normal low signal intensity Tendon(large arrow) and intermediate signal intensity palmar aponeurosis(small arrow).(B)at deeper level T1_W coronal image shows low signal intensity flexor tendons(white small arrows) passing through the carpal tunnel.the trapezium(largewhite arrow)and pisiform (black arrow) are also seen **(quoted from stoller and Brody, 1997)**

Flexor carpi-ulnaris tendon is superficial and inserts on the pisiform with fibers continue distally to form the ligamentous attachment to the hamate hook and 4th, 5th metacarpal base ***(Anderson , et al., 1998).***

Extensor tendons (FIG. 19):

The extensor tendons are stabilized by the extensor retinaculum with septations dividing the extensor tendons into six compartments, the ***1st*** compartment is located along the lateral margin of distal radius and contains the abductor pollicis longus and extensor pollicis brevis tendons, the ***2nd*** compartment is located lateral to lister's tubercle and contain the extensor carpi radials longus & brevis tendons, the ***3rd*** compartment is on the ulnar side of lister's tubercle and contain extensor pollicis longus tendon, ***4th*** compartment is located over the dorsal medial radius and contain extensor digitorum and extensor indicis proprius tendons, the ***5th*** compartment overlies the radioulnar joint and contain the extensor digiti-minimi tendon, the ***6th*** compartment lies in a dorsal ulnar groove and contains the extensor carpi-ulnaris tendon ***(Bruquist, 2003).***

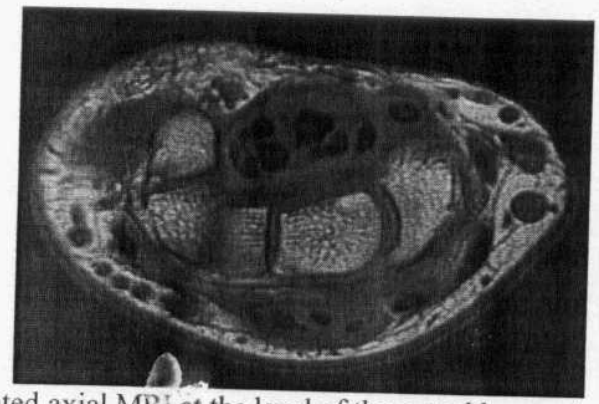

Fig.(19) T2-weighted axial MRI at the level of the carpal bones show extensor carpi radialis longus tendon, extensor carpi radialis brevis tendon, extensor pollicis longus tendon, extensor carpi ulnaris tendon & extensor tendons to digits 2-5 **(Quoted from Nadja Saupe, et al.,2005).**

Normal MRI anatomy of the wrist joint

Axial images (FIG. 20 & 21 & 22):

In the axial plane the flexor digitorum superficialis and profundus tendons are seen as tubular low signal intensity structures. In proximal sections, the flexor pollicis longus is seen deep to the median nerve. Distally, it is flanked by the adductor pollicis medially and the thenar muscles laterally, toward the thumb. At the level of the DRUJ, the volar distal radioulnar ligament is identified as a thin, low signal intensity band deep to the flexor digitorum profundus tendons . The curve of the ulnolunate ligament is demonstrated at the level of the proximal lunate and distal radius, where it follows the contour of the ulnar and volar aspect of the lunate. The palmaris longus tendon is superficial to the median nerve ***(Stoller and Brody, 1997).***

The thin low signal intensity flexor retinaculum spans the palmar border of the carpal tunnel . Its distal attachments to the hook of the lunate and tubercle of the trapezium are more reliably defined than the proximal attachments to the tubercles of the pisiform and scaphoid. The separate extensor tendons of the extensor carpi-ulnaris, extensor digiti minimi, extensor digitorum, and indicis, extensor carpi-radialis brevis, extensor pollicis longus, and extensor carpi-radialis longus are displayed from the ulnar to the radial dorsal aspect of the wrist . The Lunotriquetral (LT) and scapholunate (SL) are usually demonstrated at the level of the proximal carpal row. The arcuate ligament is seen volar to the capitate and deep to the flexor tendons ***(Totterman et al., 1993).***

The radial collateral ligament is closely applied to the radial surface of the scaphoid. The palmaris longus tendon is superficial to the median nerve and the flexor retinaculum. The two central tendons of the superficial flexor group are located superiorly within the carpal tunnel before they fan out to their insertions on the middle phalanx. On axial plane images it is possible to differentiate the four separate tendons of the flexor profundus group. The median nerve, also of intermediate signal intensity, can be identified in the superficial radial aspect of the carpal tunnel ***(Totterman et al., 1993).***

Blood vessels display low signal intensity, With gradient echo techniques, both arterial and venous structures demonstrate high signal intensity ***(Stoller and Brody, 1997).***

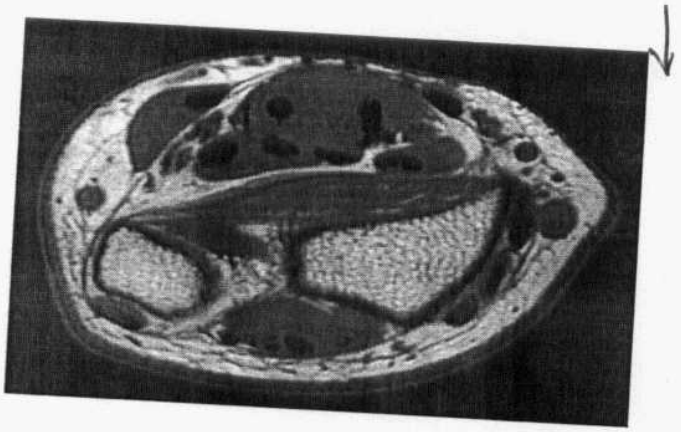

Fig.(20) T2-weighted axial MRI taken at the distal forearm show median nerve , ulnar nerveulnar artery , radial artery , flexor carpi radialis tendon &flexor carpi ulnaris tendon **(Quoted from Nadja Saupe, et al.,2005).**

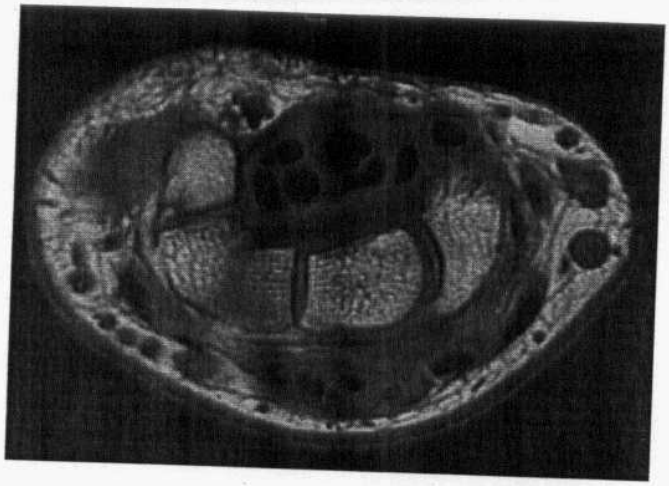

FIG.(21) T2-weighted axial MRI at the level of the carpal bones show scaphoid, capitate, hamate, triquetrum, pisiform, radial artery, ulnar artery, flexor carpi radialis tendon, flexor carpi ulnaris, flexor digitorum superficialis tendons, flexor digitorum profundus tendons, flexor pollicis longus tendon, median nerve, extensor carpi radialis longus tendon, extensor carpi radialis brevis tendon, extensor pollicis longus tendon, extensor carpi ulnaris tendon & extensor tendons to digits 2-5 **(Quoted from Nadja Saupe, et al.,2005).**

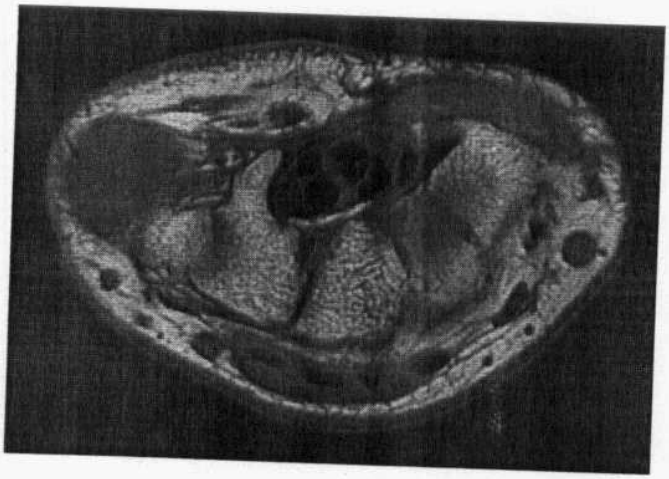

FIG.(22) T2-weighted axial MRI at the level of the carpal bones show tubercle of trapezium, trapezoid, capitate, hook of hamate, flexor retinaculum, median nerve, carpal tunnel, **(Quoted from Nadja Saupe, et al.,2005).**

Sagittal images (FIG. 23 & 24):

The sagittal imaging is especially useful in the evaluation of static instability patterns and wrist shortening and in viewing the volar to dorsal aspect of the TFC. Kienbock's fracture and fracture deformity are seen on sagittal images, complementary to coronal or axial images ***(Totterman and Miller, 1996).***

The scaphoid is identified on sagittal sections through the trapezium and more dorsally the trapezoid . The low signal intensity (RSC) ligament is represented by fibers seen along the volar aspect of the scaphoid between the volar distal radius and the distal pole of the scaphoid. The extensor pollicis longus tendon is dorsal to the radioscaphoid articulation. The pronator quadratus muscle extends along the volar surface of the radial metaphysis and distal diaphysis. The long axis (ie, vertical orientation) of the flexor pollicis longus tendon is seen at the ulnar aspect of the scaphoid. The capitate, lunate and radius are aligned in sagittal images thought the third metacarpal axis ***(Smith, 1995).***

The radiolunate ligament is located between the volar lunate surface and the distal radius at the radiolunate articulation, deep to the flexor digitorum produndus tendon. The ulnolunate ligament is radial to the TFC. The flexor digitorum superficialis and profundus tendons are best seen volar to the capitate and lunate. The ulnar limb of the arcuate ligament is seen volar to the radial aspect of the triquetrum and the ulnar aspect of the capitate. The fourth metacarpal, the hook of the hamate and the triquetrum are seen in

the same sagittal section at the most ulnar aspect of the lunate or radial aspect of the ulna. The LT interosseous ligament is also sen at this level ***(Smith, 1995).***

The TFCC is located between the lunate and the ulna and has a concave distal surface. In ulnar sagittal images, the flexor carpi-ulnaris extends in a volar direction to insert on the pisiform. The piscohamate and pisometacarpal ligaments attach to the hook of the hamate and the base of the fifth metacarpal, respectively. The intermediate signal intensity ulnar nerve is deep to the flexor carpi ulnaris. The ulnar collateral ligament component of the TFCC extends between the triquetrium and ulna, as can be seen on ulnar sagittal images out of the plane of the TFC ***(Totterman and Miller, 1996).***

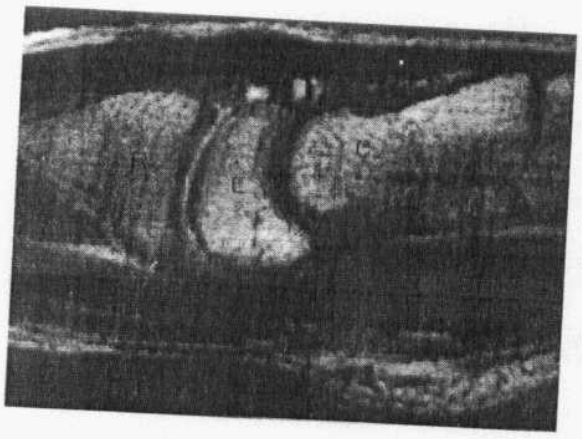

FIG.(23) Sagittal T1_weigthed MR arthrogram show lunate and aligned articulations with radius and capitate **(Quoted from Berquist, 2003).**

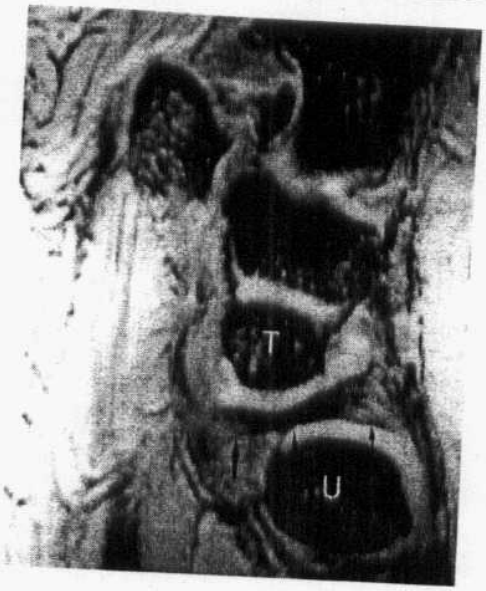

FIG.(24): Sagittal 3-D--gradient recalled echo image showing the volar radioulnar ligament (thick black arrow), the dorsal radioulnar ligament (thin black arrow), and the TFC (arrowhead). Notice the oblique position of TFC between the ulnar head (U) and triquetrum (T) and that the midportion of the TFC is thinner than its volar and dorsal portions **(Quoted from Theuman, 2002).**

Coronal images:

Coronal plane images are important in understanding the relationship between the cartilaginous and ligamentous structures of the wrist ***(Totterman and Miller, 1996).***

On volar images, the flexor retinaculum is seen superficial to the flexor tendons as a transverse band. the low signal intensity bands of the flexor digitorum tendons are seen passing through the carpal tunnel between the hook of the hamate and the trapezium. The pisohamate and pisometacarpal ligaments are shown in sections at the level of the hook of the hamate and pisiform.. The TFC is seen as a curvilinear band of low, homogeneous signal intensity. The band extends horizontally to the base of

the ulnar styloid process from the ulnar surface, of the distal radius ***(Totterman and Miller, 1995).***

The meniscal homologue has an intermediate signal intensity on T_1 and T_2 weighted images. The radioscaphocapitate (RSC) and radiolunotriquetral (RLT) ligaments are visualized volarly and extend from the radial styloid in an ulnar distal direction. These fibers are seen as parallel bands of striations. The more ulnarly located radioscapholunate (RSL) ligament is usually seen in the same plane as the RSC and RLT ligaments, and is a less substantial structure compared with the other volar extrinsic carpal ligaments. The long radiolunate (LRL) portion of the RLT ligament is represented by obliquely directed fibers extending from the volar radius to the lunate, volar to the proximal pole of the scaphoid. The SL and LT interosseous ligaments are routinely visualized on 3 mm coronal T_1 and T_2 weighted images . The extensor carpi-ulnaris tendon borders the ulnar aspect of the wrist on the same coronal sections that display the TFC and interossous ligaments. The radial collateral ligament may be partially visualized between the scaphoid and radial styloid. The articular cartilage surfaces of the carpal bones are of intermediate signal intensity on T_1 weighted images and increase in signal intensity on T_2 weighted images. On dorsal images through the carpus, the interosseous ligaments of the distal carpal row can be defined. Dorsally, the obliquely oriented extensor digiti minimi tendon on the ulnar side of the triquetrum and the extensor carpi radialis longus tendon are seen. Lister's tubercle, which contains fatty marrow, is situated between and separates the ulnar aspect of the extensor policis longus from the radial aspect of the extensor carpi-radialis previs. The dorsal interossei muscles are demonstrated between the mid carpal shafts ***(Stoller and Brody, 1997).***

Fig.(25) Coronal T2-weighted of the wrist show ulna, . radius, scaphoid, lunate, triquetrum, trapezium, trapezoid, capitate & hamate **(Quoted from Nadja Saupe, et al.,2005).**

Fig.(26) Coronal T2-weighted of the wrist show head of ulna, distal radius, articular disc of distal radio-ulnar joint, scaphoid, lunate, triquetrum, trapezium, trapezoid, capitate, . hamate, base of first metacarpal bone, flexor pollicis longus tendon, flexor digitorum profundus tendons & cephalic vein **(Quoted from Nadja Saupe, et al.,2005).**

Intravenous gadolinium:

Gadolinium remain intravascular for a short period before being distributed to intracellular fluid .Areas of inflammation, neoplasms, and other pathologic tissues enhance rapidly and retain contrast longer than normal tissues.Contrast studies are also useful for evaluating flow in patients with fractures, suspected avascular necrosis **(Berquist, 2003).**

MRI Finding in Pathological Condition

Technique of MRI wrist:

Recent studies have demonstrated that MRI had significant usefulness and impacts clinical decisions. Regarding a significant number of patient. It's demonstrated that MR studies change the clinical diagnosis in 55%, change M plan in 45%, and improve the physician's under standing of the disease process in 67% of patients ***(Hobby , et al., 2001).***

Patient position & coil selection:

Position depend on patient size, information required, soft wars & coil availability, when possible we position the patient supine with the wrist at the side, this is the most comfortable position for the patient.

The wrist can be placed over the abdomen with the elbow flexed, however the coil must be supported and separated from the abdominal wall to prevent respiratory motion artifact larger patients and children may be positioned prone or in lateral decubtus with the arm above the head.

Once the wrist is positioned it should be supported with foam pads to reduce motion and enhance comfort.

Coils for hand and wrist imaging are available n multiple configurations (Flat, circular, warp- around, partial volume and circum frontal) ***(Berquist , 2003).***

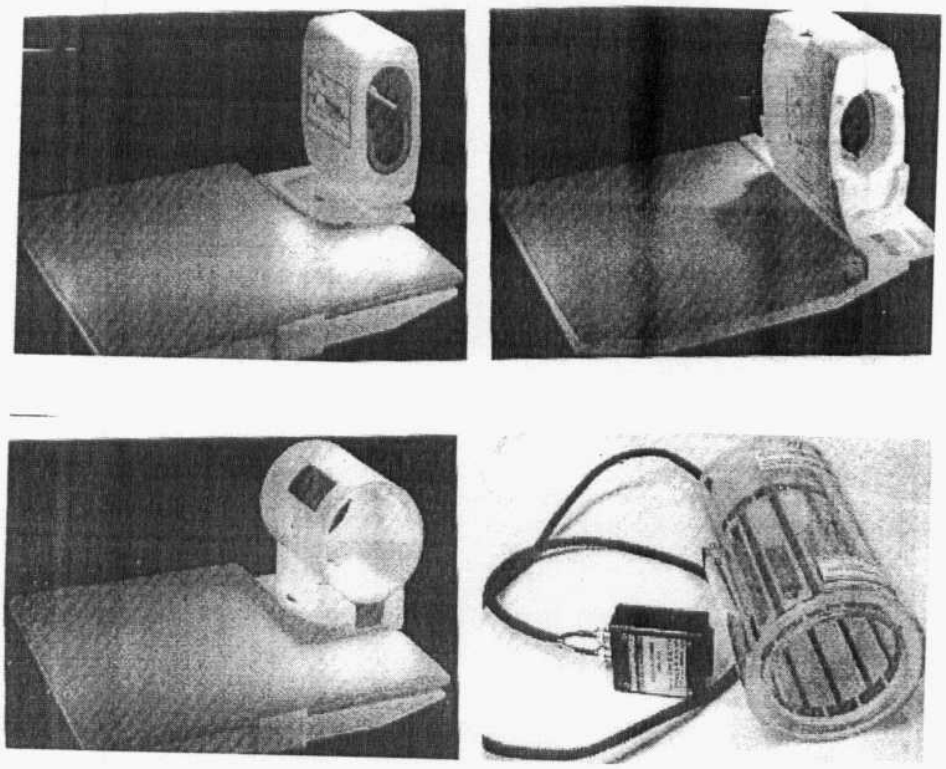

FIG.(27) Coils for hand and wrist Quadrature or phased array configuration, Four_channel phased array for wrist, Small extremity quadrature or phased array, BC_10 (Bridcage 10 cm)coil for hand and wrist at 3T. **(Quoted from Berquist, 2003).**

Protocol:

Multiplanar/ Sagittal FS/FSE/incoherent(spoiled)GRE T1:

Acts as a localizer if three plane localization is unavailable but, if the patient has been positioned correctly,may act as adiagnostic sequence.Using the body coil,medium slices/gap are prescribed on either side of the longitudinal light in the swimmer's position or on either side of the offset with the arm at the side. The area from the inferior border of the carpal bones to the distal portion of the forearm is included in the image **(Schreibman et al.,1997).**

Axial localizer :

This may prescribed from the multiplanner localizers or the Sagittal localizer. Use a surface coil to more accurately determine slice orientation for coronal imaging **(Schreibman et al.,1997).**

Coronal FS/FSE T1:

Thin slice/gap or interleaved are prescribed through the joint or ROI parallel to the proximal row of the carpus as seen from the axial localizers(the distal radioulnar joint is frequently not aligned with the carpus).displace slices inferiorly for the carpal tunnel. The area from the inferior border of the the carpal bones to the distal portion of the forearm is includedin the image**(Catherine,1999).**

Coronal FS/FSE T2 or coherent GRE T2 + chemical/spectral pre_saturation:

Slice prescription as for coronal T1.these sequences are useful for investigation the triangular fibrocartilage ,fractures or AVN. STIR is not commonly used due to poor SNR and therefore, good resolution is difficult to obtain**(Back et al., 1997).**

Axial FSE T2:

Thin slices/gap are prescribed through the ROJ orientated perpendicular to the line of the proximal carpal row as seen on the coronal images**(Catherine, 1999).**

Axial FS T1:

Slice prescription as for Axial T2. This sequence is useful for carpal tunnel syndrome and ulnar nerve lesions**(Back et al., 1997).**

Additional sequences:

Sagittal FS/FSE TI:

Thin slices/gap are prescribed orientated perpendicular to the coronal plane. This sequence is useful for localizing dorsal ganglia**(Zenetti et al.,1998)**

3D incoherent (spoiled) GRE T1 or coherent GRE T2:

used to investigate fluid or solid pathologies with thin slices 'but at the expense of resolution, Hybrid sequences showing anatomy and fluid are also popular**(Metz et al., 1996).**

Contrast medium :

Administration of intravenous gadolinium DTPA produces enhancement of tissue and subchondral hyperemia in inflammatory arthritides, Scaphoid, and lunate vascularity are studied using either a STIR, fat suppressed T2 weighted FSE coronal or fat suppressed T2weigbted intra venous gadolinium-enhanced sequence**(Stoller and Brody1997).**

Dynamic gadolinium enhanced magnetic resonance imaging (MRI) of the wrist can discriminate active from inactive RA by an intravenous bolus injection of gadolinium DTPA, 20 consecutive fast spin echo images of 3 slices of the wrist were obtained every 18 seconds**(Cimmino et al., 2003).**

Causes of wrist pain :

Causes of dorsal wrist pain	Causes of volar wrist pain
Scaphoid fracture Scaphoid impaction syndrome Fracture dislocation of carpus Lunate fracture Distal radius fracture Scapholunate ligament tear Lunotriquetral ligament tear Distal radioulnar joint injury Carpometacarpal dislocation	Carpal instability Hook of hamate fracture Kienböck's disease (acute onset)

(Bruckner and Khan, 2005)

Nerve entrapment syndrome

Carpal tunnel syndrome (CTS):-

Pathology:

Positive phalen's & tinel's signs are useful clinically, positive tinel's sign occur when tingling is noted in the nerve distributon following percussion of median nerve, phalen's sign is performed by reducing carpal tunnel volume by flexing and extending the wrist for 30-60 seconds, when positive symptoms are recreated ***(Berquist et al., 2003).***

Nocturnal symptoms are common, thenar muscle atrophy may also be evident, most patients are 30-60 yrs & women outnumber men 5:1.The condition is bilateral in 50% of patients bilateral carpal tunnel is usually occupational, but unilateral one is usually related to space-occupying lesion.

The condition is typically considered to be related to nerve compression but ischemia may also result in similar symptoms ***(Berquist, 2003).***

MRI finding:-

MR evaluation of carpal tunnel is best performed in the axial plane with wrist held neutral position **(FIG. 28)** the dimensions of carpal tunnel and the relationships between the tendons in the carpal tunnel vary with wrist position ***(Monallge et al., 1999).***

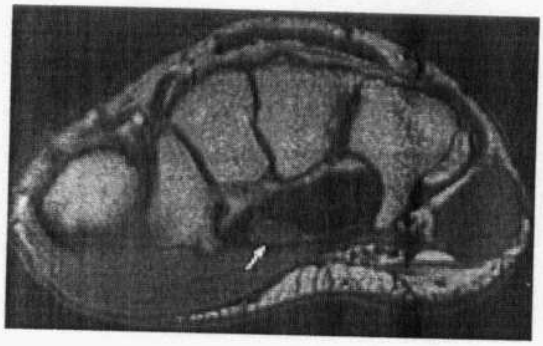

FIG.(28)the median nerve (arrow) is seen at the level of hook of hamate **(Quoted from Nadja Saupe et al., 2005).**

The nerve is typically oval in proximal carpal tunnel becoming flatter at the pisiform level and smaller in distal carpal tunnel.

In patient with carpal tunnel syndrome the nerve at pisiform level is 1.6 to 3.9 time larger than at distal radioulnar joint.

Abnormal signal intensity in the median nerve has also be described in patients CTS. The median nerve is normally higher in signal intensity than the tendons on T2-weighted sequences, abnormally high signal intensity on T2-weighted sequences has been reported in 52% to 85% of patients with CTS

Signal intensity changes are related to compression and /or ischemia, the finding of increased signal intensity in association with swelling flattening or distortion of the nerve is more significant **(FIG. 29)**. ***(Brequist, 2003).***

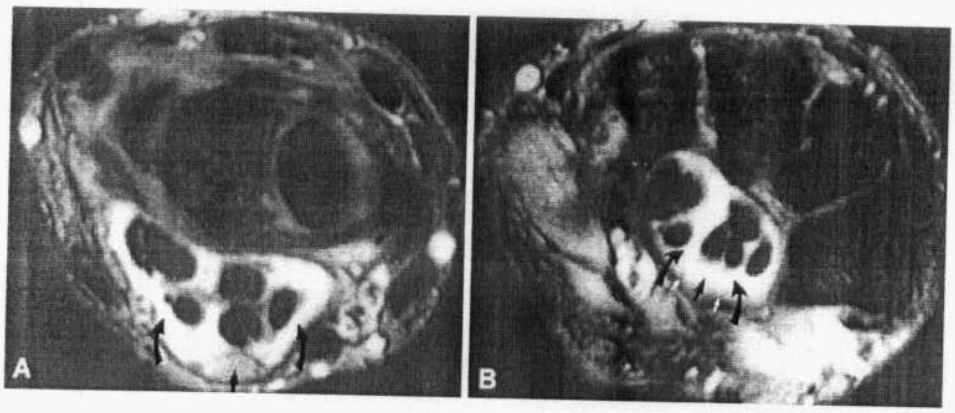

FIG.(29) In carpal tunnel syndrome, T2*-weighted axial images show **(A)** severe, high signal intensity flexor tenosynovitis (curved arrows) and swelling of the median nerve proximal to the carpal tunnel (straight arrow), and **(B)** hyperintense synovitis (curved black arrow) and hyperintense median nerve (straight black arrow). The flexor retinaculum is bowed (white arrows) **(Quoted from Theuman 2002).**

There are four major signs of CTS (**FIG. 30):**

1) focal or segmental swelling (pseudoneuroma) of the median nerve best determined by subjectively comparing the size of the nerve at the level of the distal radius with its size at the pisiform, Normally, the nerve should stay the same size or decrease distally, If the nerve is larger on progressively more distal images It is swollen.

2) Flattening or angulation of the nerve, This is best Evaluated at the distal carpal tunnel at the level of the hook of the hamate, If the nerve is compressed against adjacent' tendons and bones, the surfac e becomes faceted' or angled.

3) Bowing of the flexor retinaculum caused by increased volume of the carpal tunnel contents, This is called the bowing ratio, The bowing ratio is calculated by drawing a line from the triquetrum to the hook of the hamate on an axial image (length = TH), The distance from this line to the flexor retinaculum (palmar displacement = PD is divided by the length TB. The ratio is up to 15% in normal subjects and ranges from 14% to 26% in patients with carpal tunnel syndrome.

4) Increased signal intensity of the median nerve on T2 images may occur from obstruction of venous return from the nerve with resultant edema **(Kaplan, et al., 2001).**

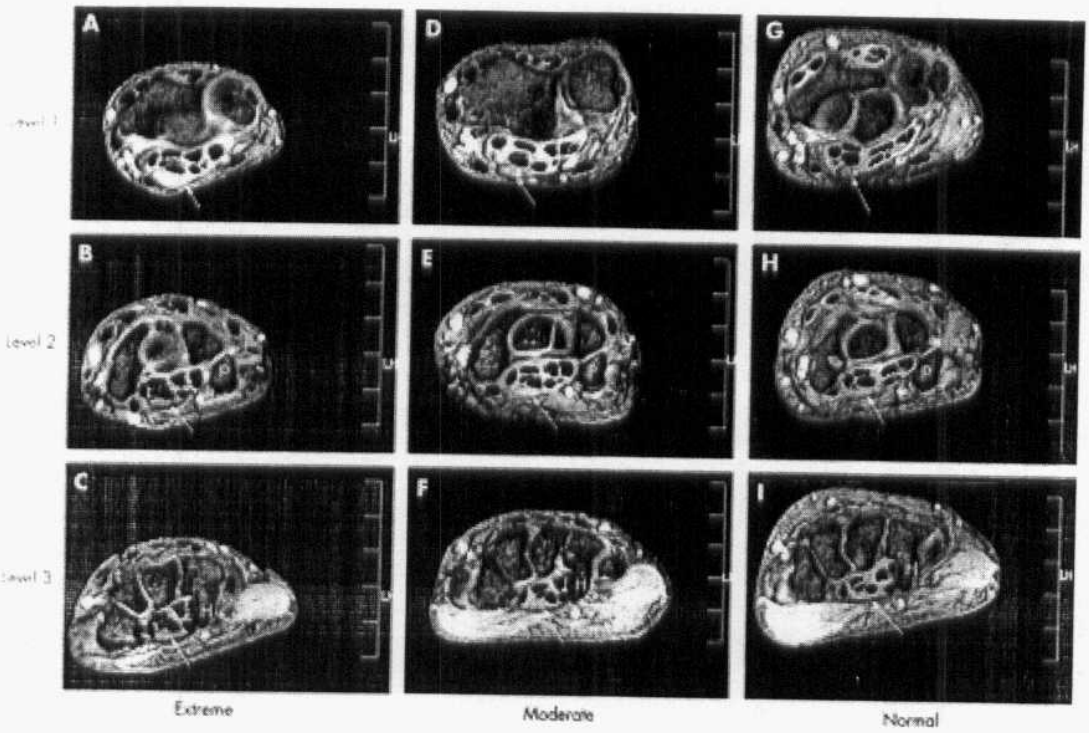

FIG.(30) T2 weighted gradient echo images, at the distal part of the distal radioulnar joint level (DRUJ) (1), at the level of the pisiform (2) and at the level of the hook of the hamate (3) in three different stages of idiopathic carpal tunnel syndrome. Solid arrow indicates the cross section of the median nerve. Upper part represents the dorsal side, and the righthand side represents the ulnar side. P, pisiform bone; H, hook of the hamate. (A–C) Extreme stage. Enlargement and high signal intensity of the flattened median nerve are seen at level 1, and enlargement of the median nerve at levels 2 and 3. Palmar bowing of the TCL is evident. (D–F) Moderate stage. Enlargement and high signal intensity of the median nerve are seen at level 2 They are slightly appreciated at level 3, and still not seen at level 1. Palmar bowing of the TCL is well appreciated. (G–I) Normal wrist **(Quoted from Uchiyama, et al., 2005).**

Tumours of median nerve e.g (fibromas and hamartoma) as well as tumour extrinsic to median nerve e.g. (ganlias and hemangiomas) produce space-occupying encroachment of carpal (**FIG.-31**) ***(Buchberger, 1997).***

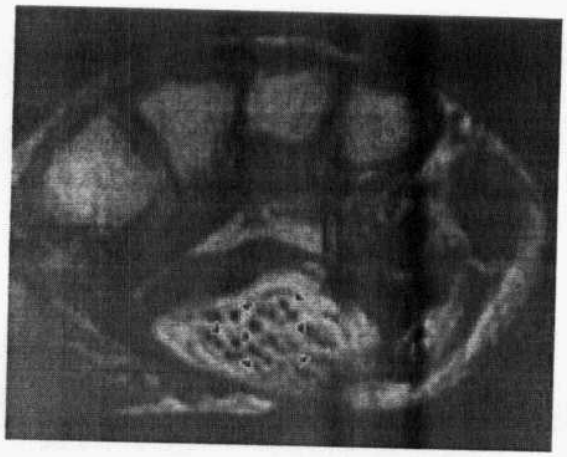

FIG.(31) Lipomatosis of the median nerve, Axial T1-weighted MR image of the wrist shows marked thickening of the median nerve with adipose tissue surrounding the nerve fascicles (arrowheads) **(Quoted from Murphey, et al., 2004).**

More important than diagnosing carpal tunnel syndrome is evalauating the cause of persistent or recurrent CTS in patients who have been treated for it surgically without success, post operative failures may be from several causes, the most common of which is incomplete release of the flexor retinaculum, (**FIG.32**). MRI also may demonstrate a persistent or recurrent mass lesion withen the carpal tunnel or development of median nerve neuroma, (**FIG.33**). The normal postoperative appearances of carpal tunnel after complete incision of the rotinaculum are the retinaculum is not visible the free ends of the retinaculum are displaced in avolar direction and the contents of the carpal tunnel are displaced in avolar direction relative to the tunnel ***(Kaplan et al., 2001).***

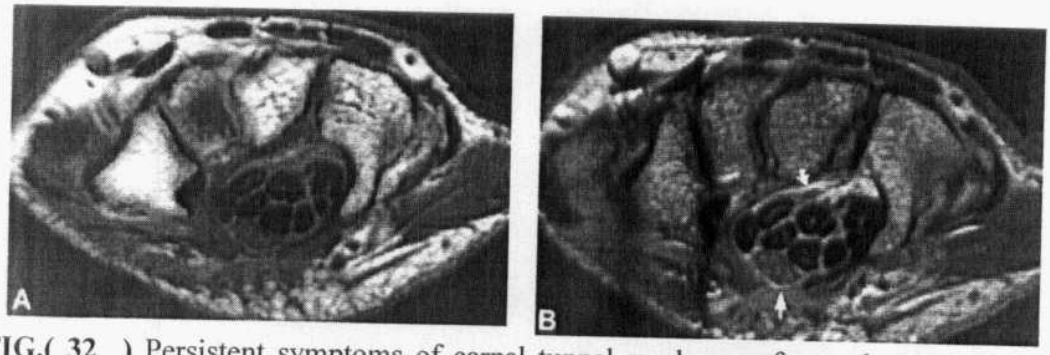

FIG.(32) Persistent symptoms of carpal tunnel syndrome after endoscopic release of the flexor retinaculum. A thin band (straight arrow) is seen overlying the enlarged median nerve on T1-weighted **(A)** and intravenous gadolinium enhanced T1-weighted **(B)** axial images. These findings are consistent with an incomplete release of the flexor retinaculum. Enhancing synovitis is also shown deep to the profundus tendons (curved arrow) **(Quoted from Stoller and Brody, 1997).**

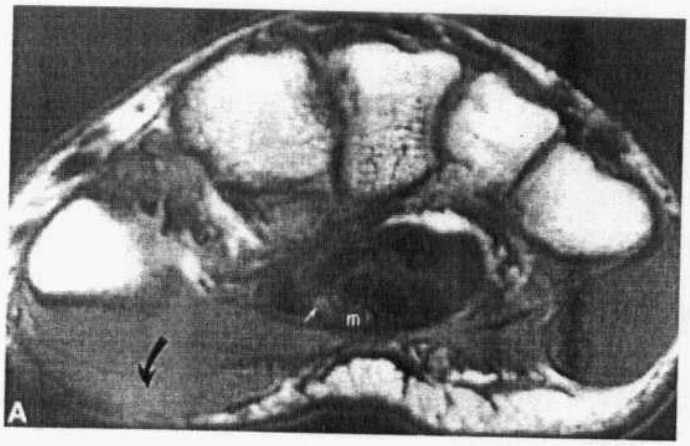

FIG.(33) Neurofibroma (small straight arrow) of the motor branch of the nerve median (m) demonstrates high signal intensity on STIR axial image**(Quoted from Stoller and Brody, 1997).**

Ulnar tunnel syndrome:-

Ulnar nerve injury or compression may occur in the elbow region, along its course or more commonly in the Guyon's canal ***(Sakai, et al., 2000).***

The canal is divided into three zones with symptome related to the zone involved.

***Zone* 1** is the proximal portion of canal before the bifurcation of the ulnar nerve injury or compression in this zone lead to motor & sensory deficits (type 1 syndrome).

***Zone* 2** includes the deep branch of the ulnar nerve, pathology in zone 2 lead to motor deficits (type 2 syndrome).

***Zone* 3** includes the superficial branch of ulnar nerve which contain primarily sensory fibers, therefore patients present with sensory deficits (type 3 syndrome).

Ulnar nerve injury or compression may be related to blunt trauma, fractures on the ulnar side of the wrist, arthropathy with calcification near pisotriquentral joint, vascular anomalies and soft tissue mass (**FIG. 34**).

Axial MRI can clearly define the anatomy pathology in the nerve or perineural tissues and muscles involvement. ***(Brequist, 2003).***

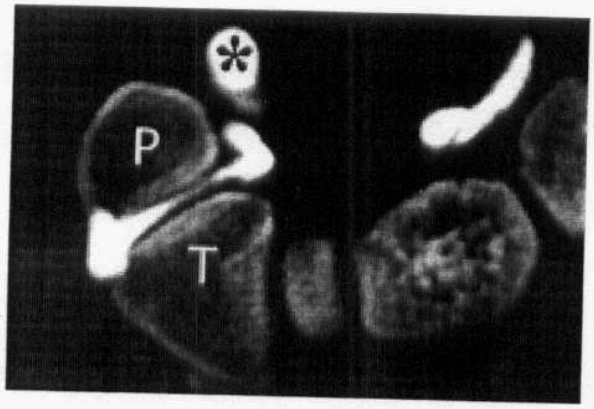

FIG.(34) Guyon tunnel syndrome in a 54-year-old man with a pisotriquetrum ganglion, Axial CT arthrogram show a rounded ganglion (*), which displaces the ulnar artery (curved arrow) and compresses the ulnar nerve (straight arrow) against the pisiform (*P*). *T* = triquetrum **(Quoted from Murphey, et al., 2004).**

Ligamentous lesion

Pathology:

Scapholunate (SL) and lunotriquetral (LT) ligaments are the two intrinsic carpal ligaments of greatest clinical significance, disruption of these ligaments may cause instability and pain ***(Kaplan et al., 2001).***

Scapholunate (SL) ligament tear:

The normal appearance of the scapholunate ligament varies with the portion included in the image plane, the ligament is C-shapled extending from the dorsal to proximal to volar aspects of scapholunate articulation ***(Brequist TH, 2001).***

The abnormalities on MRI that indicate SL ligament abnormality are (1) discontinuity of the ligament with or without increased space between scaphoid & lunate bones (**FIG. 35**) (2) complete absence of scapholunate ligament (3) distorted morphology with fraying, thinning and irregularity (4) elongated ligament with an increased intracarpal space the accuracy of MRI has been reported as 90% when compared with arthrography and 95% when compared to surgery (arthoscopy & arthrotomy) ***(Kaplan et al., 2001).***

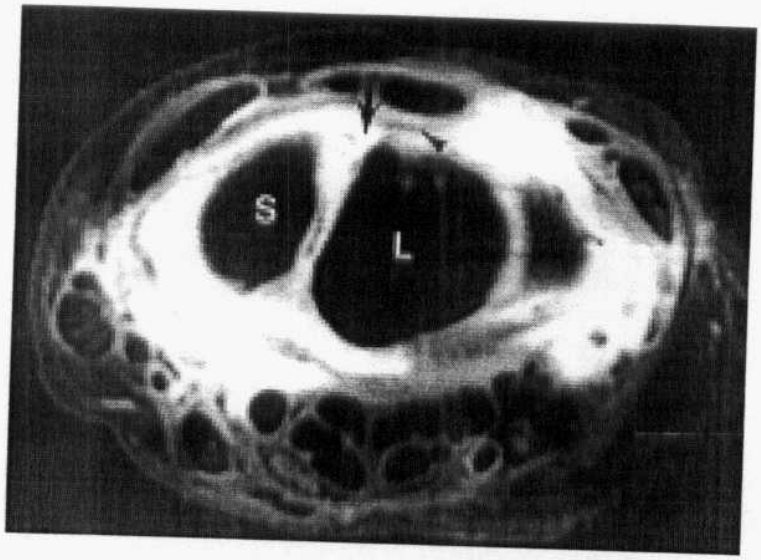

FIG(35) — Wrist of 54-year-old man with abnormal scapholunate ligament of left wrist S = scaphoid bone, L = lunate bone. Axial T1-weighted MR image with fat saturation obtained after intraarticular gadolinium administration shows abnormal discontinuity (*arrow*) of dorsal aspect of scapholunate ligament. Note intact dorsal radiotriquetral ligament (*arrowhead*) **(Quoted from Totterman and Miller, 1996).**

Totterman and miller (1996) described the (SL) ligament appearance in volar, middle and dorsal planes on caronal three-dimensional gradient echo images, the volar portion of the ligament is trapezoidal with inhomogenous signal intensity on MR images, the mid portion (proximal of (SL) ligament is triangular with inhomogenous low to intermediale signal intensity, the dorsal portion of the ligament is band like with inhomogenous low to intermediate signal intensity (**FIG.36**) ***(Totterman and Miller, 1996).***

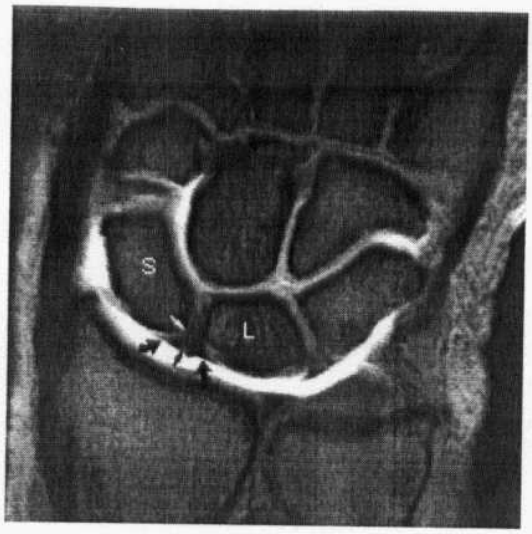

FIG.(36) Normal variations in the appearance of the scapholunate ligament. There is intermediate signal intensity hyaline cartilage at the SL interface with the scaphoid (white arrow) and not the lunate bone. Low to intermediate linear signal intensity (black arrow) traverses both the proximal and distal surfaces of the SL ligament without tear. The proximal base of the SL ligament extends past the inflection points of both the scaphoid and lunate bones (curved arrow) (fat-suppressed T1-weighted coronal MR arthrogram). S, scaphoid; L, lunate **(Quoted from Stark and Bradly, 1999).**

Lunotriquetral ligament tear

Disruption of the lunotriquteral ligament is not as easy to diagnose as that of the scapholunate ligament, because of its relatively smaller size. Similar abnormalities to those seen in an abnormal scapholunate ligament are present in an abnormal lunotriquetral ligament **(Fig. 37 A&B).** Tears of the lunotriquetral ligament are the second most common causes of carpal instability and result in the lunate tilting in a volar direction (volar intercalated segmental instability, or VISI). There is a strong association between tears of the triangular fibro cartilage and lunotriquetral ligament tears ***(Kaplan et al., 2001).***

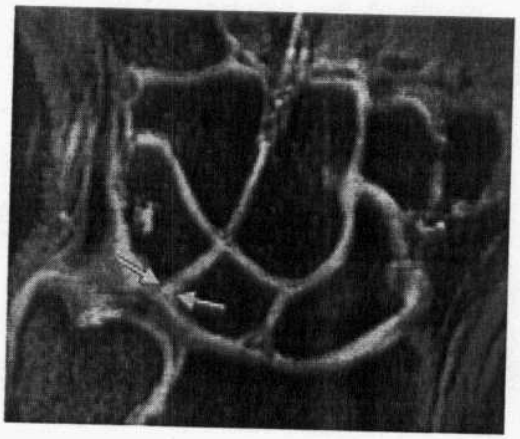

FIG.(37- A) Images in two different patients with torn lunotriquetral ligaments. Coronal three-dimensional gradient-echo indirect MR arthrogram in a 33-year-old man illustrates abnormal high signal intensity (arrows) through the region of the lunotriquetral ligament **(Quoted from Haims, 2000).**

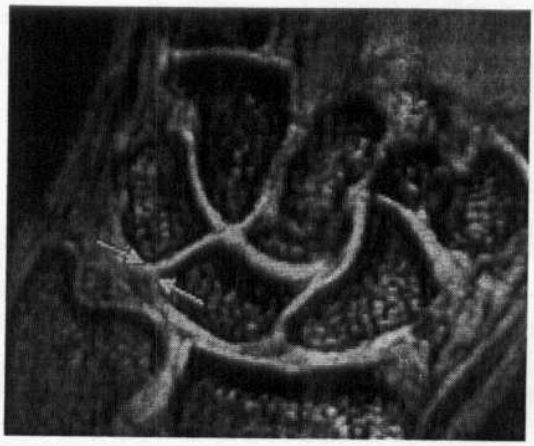

FIG.(37- B) Images in two different patients with torn lunotriquetral ligaments. Unenhanced coronal three-dimensional gradient-echo MR image in a 46-year-old man demonstrates abnormal high signal intensity in the region of the lunotriquetral ligament (arrows) **(Quoted from Haims, 2000).**

The improved accuracy of MRI for the demonstration of SL tears compared with LT tears reflects the greater difficulty in imaging the smaller LT ligament ***(Strak and Brdly, 1999).***

MR arthrography has increased the accuracy of evaluation of SL and LT ligament tears, especially in peripheral ligament avulsions where the ligament has not lost its normal morphology. These tears may be difficult to detect n routine MR gradient-echo, STIR, or fat-suppressed T_2-weighted FSE images unless there is a fluid interface identified between the torn ligament and corresponding osseous attachment ***(Cerezal et al., 2002).***

Triangular fibrocartilage complex (TFCC) abnormalities

Arthrography is consided as the gold standard technique for diagnosis of TFCC tears, most authers would agree that MRI is equivalent to arthrography with spicificaties and sensitivities ranging from 75% to 100% ***(Keogh et al., 2004).***

TFCC tears can result in ulnar sided pain, weakness, an crepitus, TFC tears have been classified into two types traumatic (class I) and degenerative (class II). The tears are subdivided further by location into radial and ulnar tears, class IA tears (**FIG. 38** .) involve the radial side of the disk and usually are slit like, class IB tears (**FIG. 39**) are avulsions of TFC from ulna, an avulsion of the ulnar attachment with injury of ulnocarpal ligaments is classified as class IC lesion (**FIG. 40**) class ID tears (**FIG.41**) are avulsion of the radial attachment . Degenerative tears are classified on the basic of severity with class IIA lesion being the least severe with thinning of the TFC and class IIE lesion being the most severe with TFC perforations, osteoarthritis and ligamentous disruptions ***(Georges , et al., 2003).***

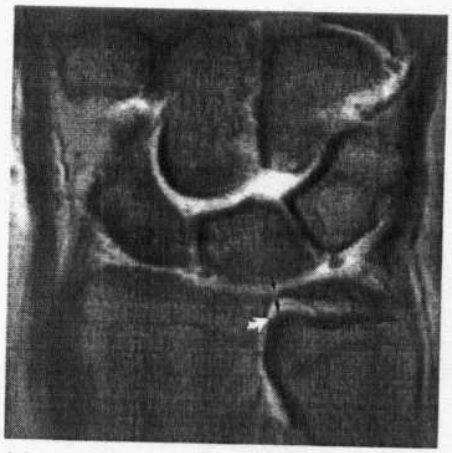

FIG.(38) Class IA lesion with slit-like tear (straight arrow) of the radial aspect of the TFC medial to its radial origin.There is communication of radiocarpal joint contrast (curved arrow) with the distal radioulnar joint**(Quoted from Stoller and Brody, 1997).**

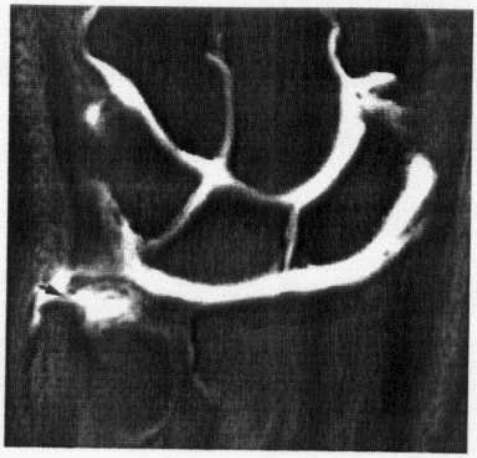

FIG.(39) Class IB lesion with traumatic avulsion of the ulnar attachment of the TFC. There is direct extension of contrast between the ulnar styloid and the avulsed TFC (arrow) (fat-suppressed T1-weighted coronal arthrographic image). In addition, this patient has an avulsion of the ulnar aspect of the SL ligament and absent LT ligament**(Quoted from Stoller and Brody, 1997).**.

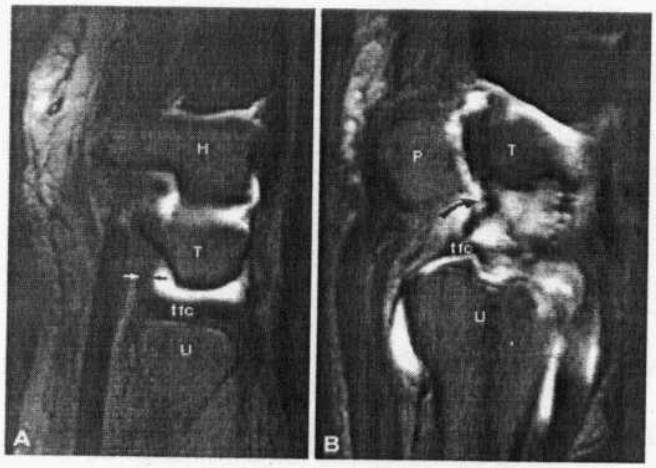

FIG.(40) Fat-suppressed T1-weighted sagittal MR arthrographic images comparing (A) intact (black and white straight arrow) ulnocarpal (ulnolunate and ulnotriquetral) ligament with (B) avulsed osseous insertions (curved arrow) of the ulnocarpal ligaments. There is also associated tearing of the dorsal radial aspect of the TFC. Isolated avulsion of the distal ulnolunate or ulnotriquetral ligaments as described in a class IC lesion is not common. H, hamate; T, triquetrum; tfc, triangular fibrocartilage; U ،ulna; P, pisiform**(Quoted from Stoller and Brody, 1997).**

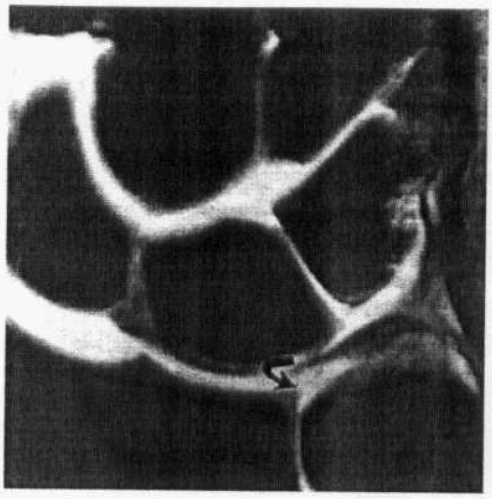

FIG.(41) Traumatic avulsion of the radial attachment of the TFC as described in class ID lesions. Note the exposed articular cartilage at the radial sigmoid notch. Fluid communicates between the radiocarpal and distal radioulnar compartments (curved arrow) on this fat-suppressed T1-weighted coronal MR arthrographic image. The LT ligament is absent**(Quoted from Stoller and Brody, 1997)**.

Class II degenerative lesions demonstrate the spectrum of ulnocarpal abutment syndrome findings. Class IIA injuries represent TFCC wear (**Fig. 42**). Class IIB injuries include TFCC wear with associated lunate and/or ulnar chondromalacia (**Fig.43).** Class IIC injuries represent a TFCC perforation in association with lunate or ulnar chondromalacia (**Fig. 44**). Class IID lesions (**Fig. 45**) include a TFCC perforation, lunate or ulnar chondromalacia, and an LT ligament perforation. In class IIE injuries (**Fig. 46**) there is the additional finding of ulnocarpal arthritis **(Stoller and Brody, 1997).**

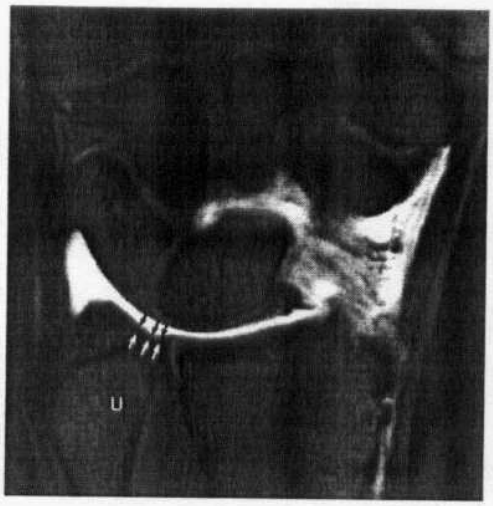

FIG.(42). Class IIA lesion with degenerative thinning (arrows) of the TFC without perforation. No lunate chondromalacia is present and the LT ligament is intact. Fat-suppressed T1-weighted coronal MR arthrographic image. U, ulna **(Quoted from Stoller and Brody, 1997).**

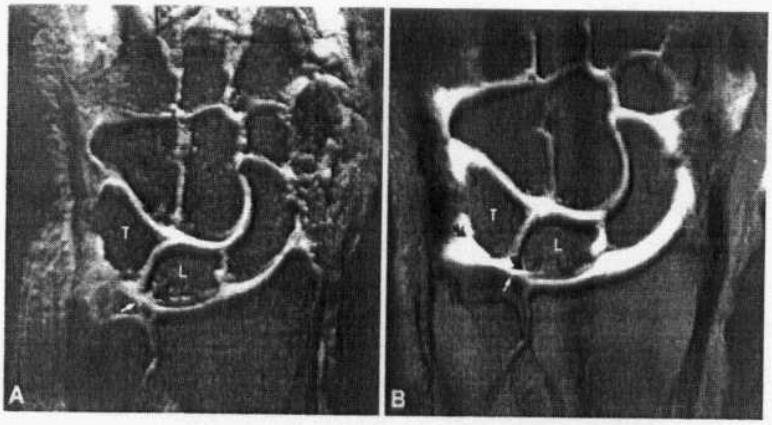

FIG.(43) Class IIB lesion with degenerative fraying of the distal aspect of the TFC (straight arrow). There is chondromalacia of the lunate and triquetrum (curved arrow) without associated TFC perforation. The LT and SL ligaments are torn (A: T2*-weighted coronal image; B: fat-suppressed T1-weighted coronal MR arthrographic image**(Quoted from Stoller and Brody, 1997).**

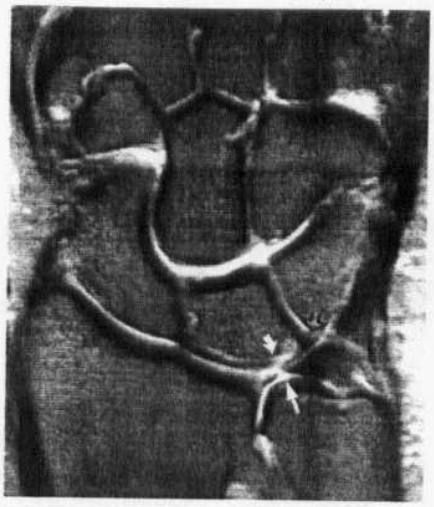

FIG.(44) Class IIC lesion with central TFC perforation (straight arrow) and lunate chondromalacia (curved arrow) on a fat-suppressed T2-weighted fast spin-echo coronal image. No intraarticular contrast was required to facilitate the diagnosis. The LT ligament is intact (open arrow). Tapering of the edges of the TFC is seen in degenerative (class II) lesions whereas traumatic (class I) tears tend to have abrupt or straight margins**(Quoted from Stoller 1997)**.

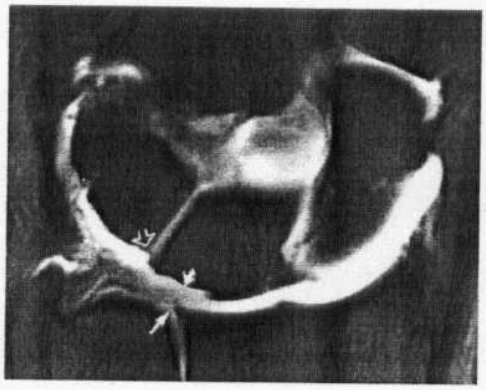

FIG.(45) Fat-suppressed T1-weighted coronal arthrographic image demonstrating class IID injury with perforation of TFC (straight arrow), loss of lunate articular cartilage (curved arrow), and lunotriquetral ligament disruption (open arrow). The intrasubstance enhancement of the TFC is commonly seen in degenerative lesions **(Quoted from Stoller and Brody, 1997).**

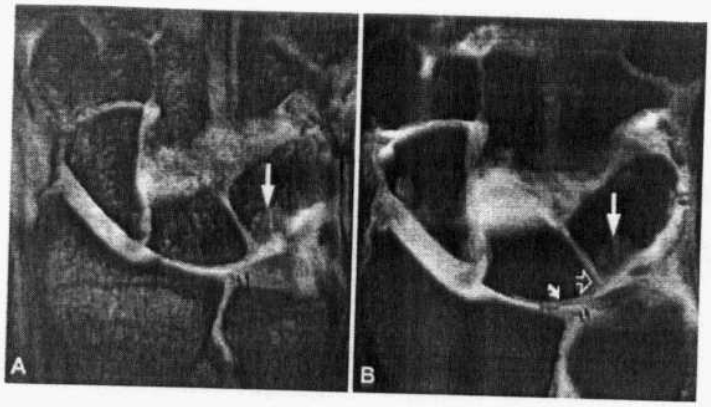

FIG.(46) Class IIE lesion with ulnocarpal arthritis demonstrates a central TFC perforation (small straight arrows), lunate (curved arrow) and triquetral chondromalacia, lunotriquetral ligament tear (open arrow), and triquetral subchondral erosion (long straight arrow) (A: T2*-weighted coronal image; B: fat-suppressed T1-weighted coronal arthrographic image**(Quoted from Stoller and Brody, 1997)**.

TFCC is visualized best on coronal images, the TFC component is normally a low signal intensity, disk like structures, but it may show intermediate signal foci on T_1 weighted image because of myxoid degeneration.

Complete tears or perforation of TFC appear as region of high signal on T_2-weighted image that extend from radiocarpal joint to the distal radioulnar joint, traumatic tears are more common at radial attachment, partial tears are seen as focal region of high signal on T2-WI that affect only the radiocarpal or the distal radioulnar surface of the disk***(Georges, et al., 2003).***

Unlar impaction syndrome

The ulnolunate impaction syndrome is a pain that occurs because of chronic abutment of the distal ulna against the proximal lunate. There is a strong association between ulnar plus variance leads to altered and increased forces transmitted across the ulnar side of the wrist. Ulnar plus variance may be a congenital variant or may be develop as the result of an impacted distal radial fracture ***(Steinborn, et al., 2003).***

Ulnolunate abutment syndrome begins with degeneration of the TFCC without tear. Next, chondromalacia of the ulnar head and proximal lunate develop (**FIG. 47**) . Later, there are central TFCC tears. LT tears and progressive a reticular degeneration of the ulna and lunate follow. In the final stage, there are degenerative changes within the distal radioulnar joint. Patients have chronic ulnar wrist pain, clicking, or both symptoms (**FIG. 48**) ***(Cerezal, et al., 2002).***

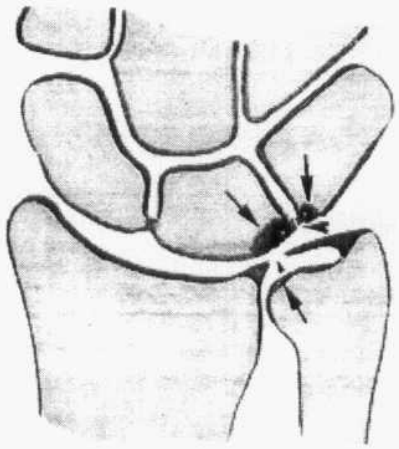

FIG.(47) Diagram illustrates the full spectrum of pathologic conditions in ulnar impaction syndrome, including chondromalacia of the ulnar head, the ulnar side of the lunate bone, and the radial side of the triquetral bone (arrows); central perforation of the TFC (small arrowhead); and lunotriquetral ligament tear (large arrowhead)**(Quoted from Cerezal, et al., 2002)**

(A) **(B)**

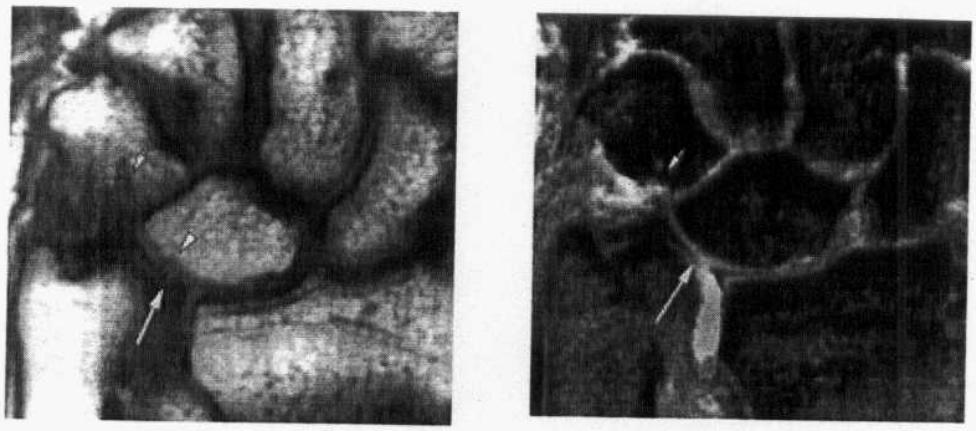

Fig.(48) Ulnar impaction syndrome in a 32-year-old woman with significant positive variance and insidious onset of ulnar-sided pain Coronal T1-weighted (repetition time msec/echo time msec = 500/15) **(A)** and gradient-echo **(B)** MR images show marked positive ulnar variance, central perforation of the TFC (long arrow), and chondromalacia of the lunate bone (arrowhead in a) and triquetral bone (short arrow). An arthroscopic "wafer" procedure was performed, with excellent results**(Quoted from Cerezal, et al., 2002)**.

MRI provides an excellent modality for visualizing the full spectrum of the abnormalities of the ulnolunate abutment syndrome MRI may demonstrate a long ulna, although precise measurements are problematic. MRI can also demonstrate subchondral cystic changes (**FIG.49**) .and subchondral sclerosis in the lunate . There may also be an associated tear of the LT ligament and associated central perforation of the TFCC ***(Steinborn, et al., 2003).***

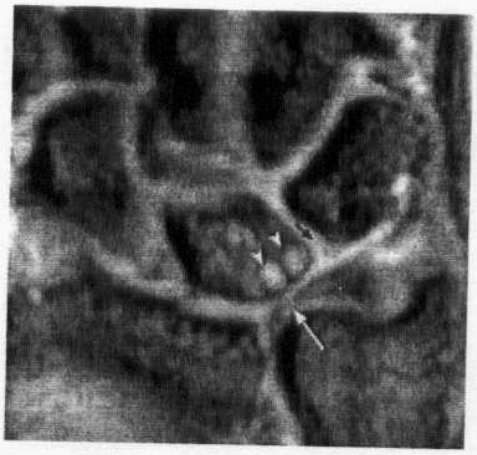

Fig.(49) Ulnar impaction syndrome in a 41-year-old man with positive variance and chronic ulnar-sided wrist pain. Coronal gradient-echo MR image reveals central TFC perforation (white arrow), subchondral cystic changes in the lunate bone (arrowheads), and a lunotriquetral ligament tear (black arrow) **(Quoted from Cerezal et al., 2002)**.

Distal radioulnar joint impaction

The distal radioulnar joint is formed between the semicircular convex ulnar head and the ulnar convexity in the distal radius-sigmoid notch. Stability for this joint is provided by the interosseous membrane and to a greater extent by the triangular fibrocartilage complex. The diagnosis of distal radioulnar joint sublaxation can be difficult. Symptoms and physical exam. are often nonspecific and conventional radiographs are generally unreliable ***(Timins et al., 1996).***

When the wrist is pronated, the ulna moves dorsally, and when the wrist is supinated, the ulnar head moves in a volar direction. When evaluating distal radioulnar joint instability, it is optimal to include axial

images of both wrists in pronation, supination and neutral positioning . These images are obtained with the arms above the patients head with the wrists placed in a head or neck coil. T1- weight images provide a fast and accurate method for determination of distal radioulnar joint instability. MR imaging has an advantage for demonstrating soft tissue abnormalities including triangular fibrocartilage tears, which may be associated with distal radioulnar joint instability (**FIG. 50**) ***(Kaplan et al., 2001).***

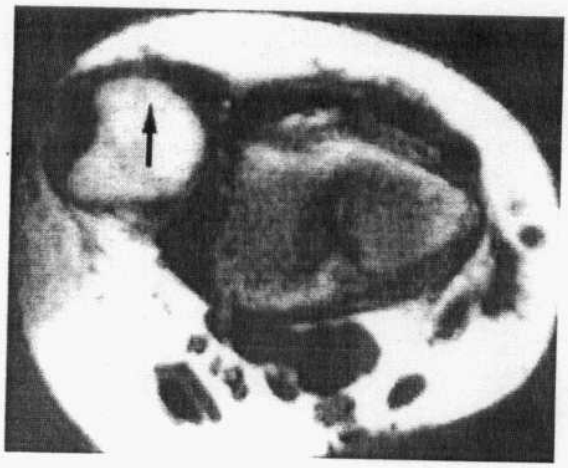

FIG.(50) T1-weighted axial image shows dorsal displacement of the ulna (arrow). The ulnar attachment of the volar radioulnar ligament is not seen**(Quoted from Stark and Bradly, 1999)**.

Tendon abnormalities

Injuries to the tendons of hand and wrist occur commonly. Inflammation of the tendon (tendonitis) or tendon sheath (tenosynovitis) or perivascular bundle (peritendonits) may occur alone or in combination. tendenosis is a degenerative process seen with overuse and age that result in mucoid degeneration, vascular ingrowth and cartilage metaplasia.

Normal tendons are low signal intensity on all MR sequences, there is normally minimal fluid in the tendon sheath, when fluid completely surrounds the tendon, inflammation is likely, inflammatory changes in the tendon sheath and tendon are most easily demonstrated on T2-weighted sequences ***(Girgrs , et al., 2000).***

Tendon sublaxation / dislocation

Tendon abnormalities may present as complete rupture or as partial tear, on MRI, complete tear show discontinuity of tendon with free edges, partial tear appear as linear high intrasubstance signal on T2_WI, increased signal withen the tendon substance and thickening of tendon indicate degenerative changes ***(Georges , et al., 2003).***

Sublaxation or dislocation of the tendons in the hand and wrist may occur with acute trauma, previous fracture. with osseous deformity, inflammatory arthropathies and overuse syndromes. Patient may present with pain swelling and reduced function depending on tendon or tendons involved ***(Swen , et al., 2000).***

Imaging should include radiographic screening to evaluate osseous structure, joint deformity and areas of soft tissue swelling, U/S or MRI can be employed to evaluate tendon position **(FIG. 51)**.

MRI can be obtained using T_1 & T_2- weighted sequences, the axial plane is often most useful, usually coronal or sagittal images are added depending on the tendon involved ***(Brequist, 2003).***

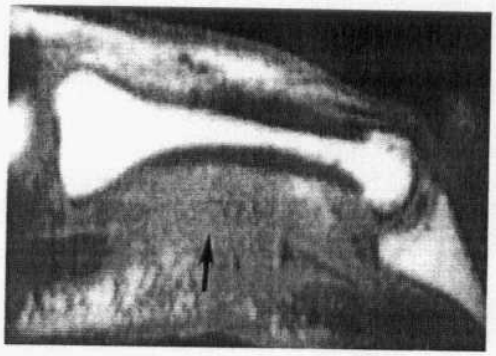

FIG.(51) T1-weighted sagittal image show Complete disruption of the flexor digitorum superficialis and profundus tendons (arrow) are seen **(Quoted from Stoller and Brody, 1997)**.

Inflammatory disorders

Inflammatory disorders involving the tendons are common, tendonitis or tenosynovitis of the first dorsal compartment (de Quervian's tenosynovitis) ***(Chein et al., 2001).***

Extensor carpi ulnaris (ECU) tendon is the second most common location for tenosynovitis stensoing ***(Huang and Strauch, 2000).***

De Quervian's tenosynovities involve the first dorsal compartment, patients present with pain and restriction of extensor pollicis brevis and abductor pollicis longus, up to 77% of patient are women involved in nursing, secretarial work or other occupations resulting in overuse symptoms ***(Chein , et al., 2001).***

MRI finding in De Quervain syndrome may have a varied appearance, there may be obliteration of subcutaneous fat surrounding the tendon, with tendons surrounded by intermediate signal intensity tissue on all pulse sequence, or there may be tenosynovitis with high signal fluid surrounding them on T_2. W images, the tendons may be normal in caliber or thickened, or there may be high signal with the tendons from partial tears or degeneration (**FIG. 52**) ***(Anderson, et al., 1998).***

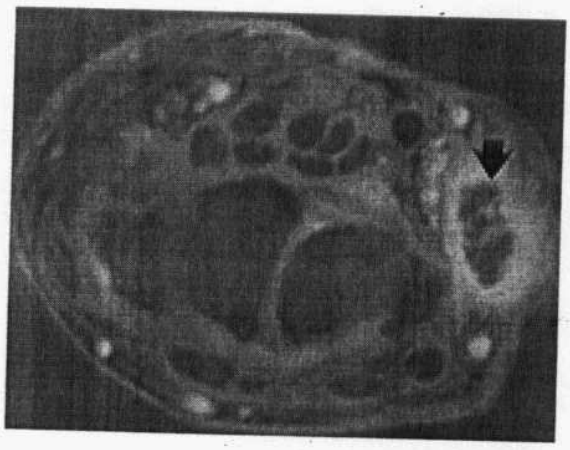

Fig.(52) De Quervain stenosing tenosynovitis. Indirect axial MR arthrographic image of the wrist (600/10) demonstrates enhancement in the first extensor compartment (arrow), a finding that is consistent with De Quervain stenosing tenosynovitis**(Quoted from, Steinborn, et al., 2003).**

ECU tendon is commonly involved with tenosynovitis or partial tears, this may occur secondary to repetitive Sublaxation or dislocation which occur when the ECU tendon sheath has been disrupted from an injury to the TFCC. We only diagnose tenosynovitis or partial tendon tears of the ECU tendors when there is fluid surrounding the entire tendon, or the tendon is abnormally thick or thin (**FIG. 53**). High signal intensity withen this particular tendon is not enough to call an abnormality because, it's present in many asymptomatic individuals ***(Kaplan et al., 2001).***

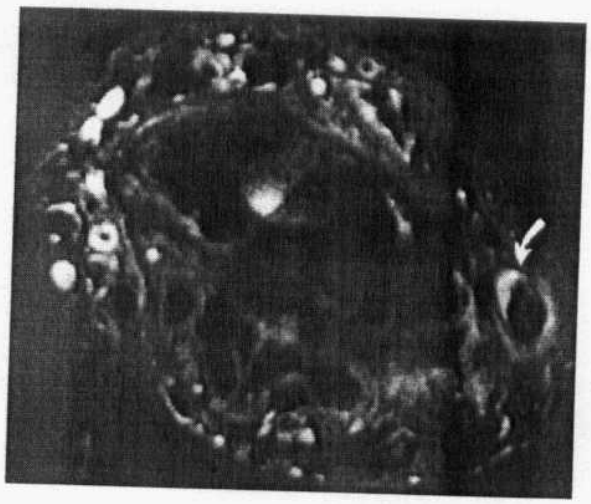

FIG.(53) Tenosynovitis of the extensor carpi ulnaris tendon of the sixth dorsal compartment is shown as fluid hyperintensity of the tendon sheath (arrow) on STIR axial image.**(Quoted from Stark and Bradly, 1999).**

Avascular bone necrosis

Pathology:

The two most common sites, for osteonecrosis in the wrist are the proximal pole of scaphoid after fractures and lunate bone, rarely the proximal portion of capitate may undergo osteonecrosis after being fractured ***(Herneth et al., 2001).***

A vascular necrosis (AVN) of scaphoid:

Injuries to the wrist often occur as a result of a fall on the outstretched hand. The most common acute injuries are fractures of the distal radius(**Fig. 54)** or scaphoid bone, or ligament tears**(Brcukner and Khan, 2005)**.

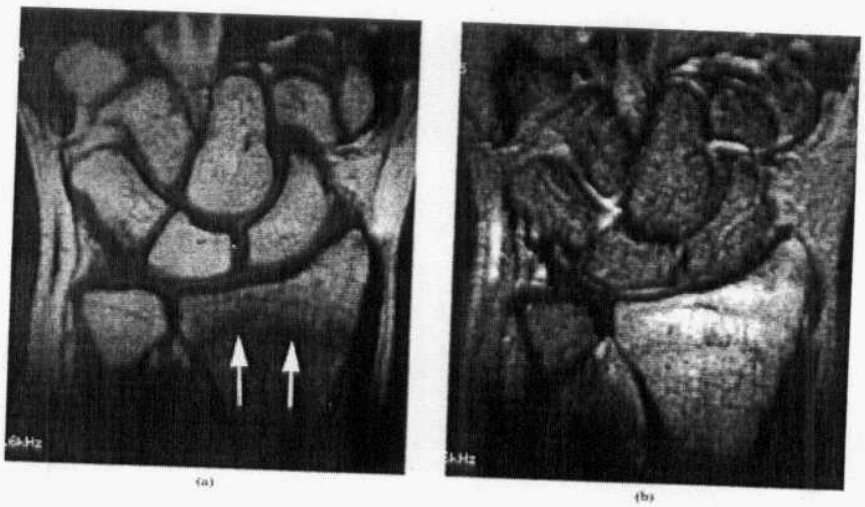

Fig.(54) (A) Coronal T_1 weighted image demonstrating a low signal fracture line (arrows) of the distal radius that was radiographically occult. **(B)** Same patient as (A). Coronal short tau inversion recovery image demonstrating high signal surrounding the distal radius fracture indicating marrow oedema and haemorrhage.**(Quoted from McAlinden , 2001).**

Avascular necrosis of the scaphoid is primarily posttraumatic event that occurs secondary to proximal pole or waist fractures that endanger the dominant blood supply of the scaphoid (**Fig. 55).** there is often sclerosis of the proximal pole relative to osteopenia and hyperemia of adjacent nonnecrotic bone. By the time sclerosis, resorption, and collapse are evident on plain film radiographs, however, the disease in an advanced state. When AVN of the scaphoid occurs in the absence of fracture, it is called Preiser's disease (**Fig. 56)** ***(Ikeda and Oka, 2000).***

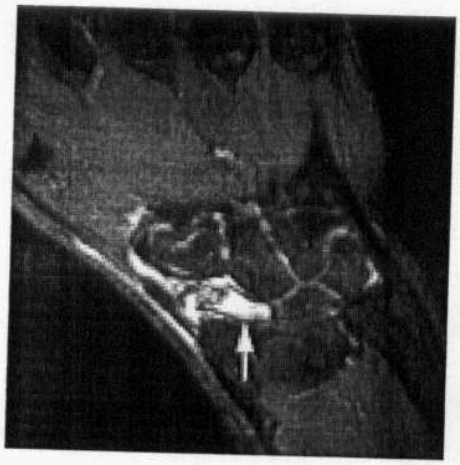

FIG.(55) Coronal short tau inversion recovery image demonstrating high signal throughout the scaphoid (arrow) indicating a fracture.**(Quoted from McAlinden , 2001).**

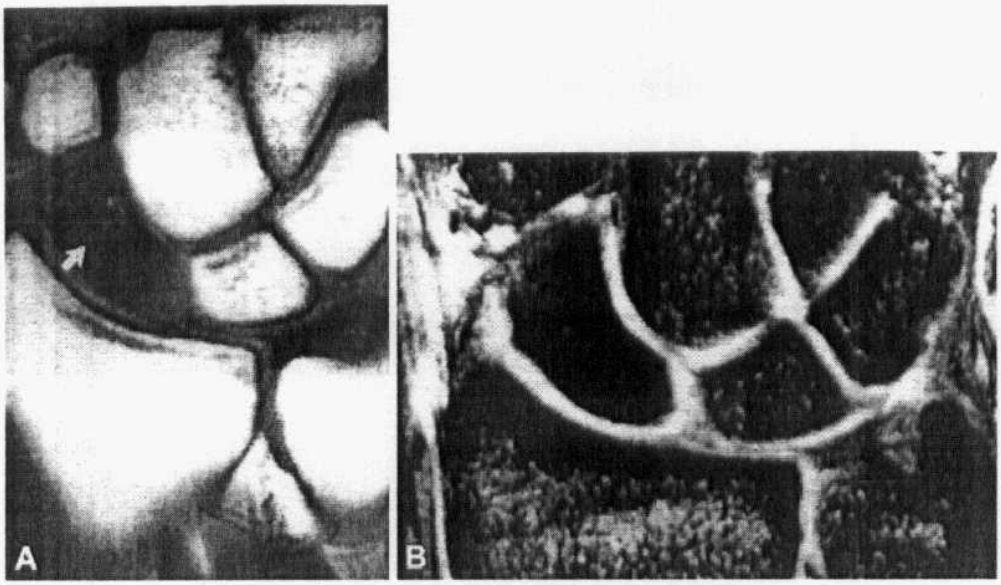

Fig.(56) Preiser's disease (A) Coronal T1_WI show low signal intensity sclerotic scaphoid (arrow) without an identifiable fracture site.(B) Coronal T2*_WI dose not show icreased signal intensity **(Quoted from Stoller and Brody, 1997).**

The application of MR imaging for detection and evaluation of AVN is facilitated by the bright signal intensity contrast generated from the normal fatty marrow content of the carpal bones. MR imaging has been reported to be as sensitive as bone scintigrtaphy in the detection of AVN, and even more specific. On T_1-weigthed sequences, MR sensitivity rates for the detection of deceased marrow signal associated with AVN are 85.5%. With the addition of T_2-weighted sequence, specificity is reported to be 100% (**Fig. 57**) ***(Stark and Bradly, 1999).***

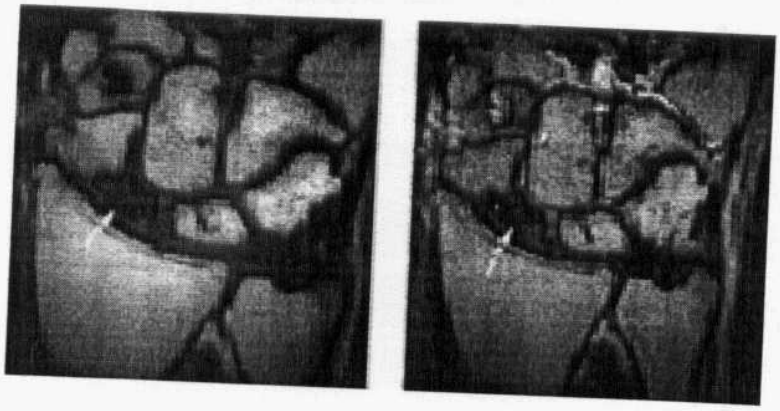

Fig.(57) Coronal **(A)** T_1 and **(B)** T_2 weighted images, respectively, demonstrating low signal in the proximal pole fragment of the scaphoid consistent with avascular necrosis**(Quoted from McAlinden 2001)**

The most common MR appearance of AVN of the scaphoid is low signal intensity in the proximal pole on both T_1-weighted and T_2 weighted imaging **(Fig. 58).** In diffuse marrow necrosis, low signal intensity marrow may not be restricted to the proximal pole. T_2 weighted images may demonstrate localized fluid accumulation and limited marrow edema of the proximal pole.

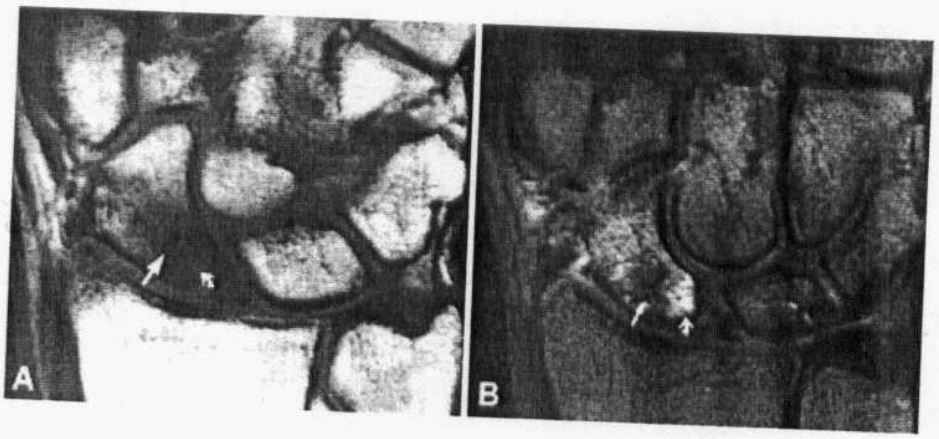

Fig.(58) Scaphoid fracture avascular necrosis(curved arrow)of the proximal pole which has low signal on coronal T1_ WI **(A)** and high signal on hyperemic viable bone on fat Suppressed coronal T2_WI **(B)** .the fracture line (atraight arrow) has low signal on both Pulse sequences **(Quoted from Stark and Bradly, 1999).**

Reactive marrow hyperemia of the distal pole may be confused with diffuse changes of necrosis. Short T_1-weighted inversion recovery images can be used to document increased hyperemia of the distal pole marrow as well as proximal pole vascularity, which may not be appreciated on T_1-, T_2-, or T2*-weighted images **(Fig. 59) &(Fig. 60)**.

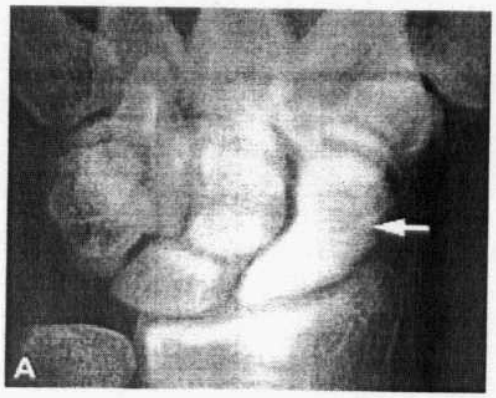

Fig.(59) An anteroposterior radiograph shows diffuse sclerosis of the scaphoid. The deformity of the proximal aspect of the proximal pole is known as the "nipple sign" and is sometimes seen in association with scaphoid fractures. There is relatively little sclerosis of the distal pole (arrow) when compared with that present in the proximal pole**(Quoted from Stoller and Brody, 1997).**

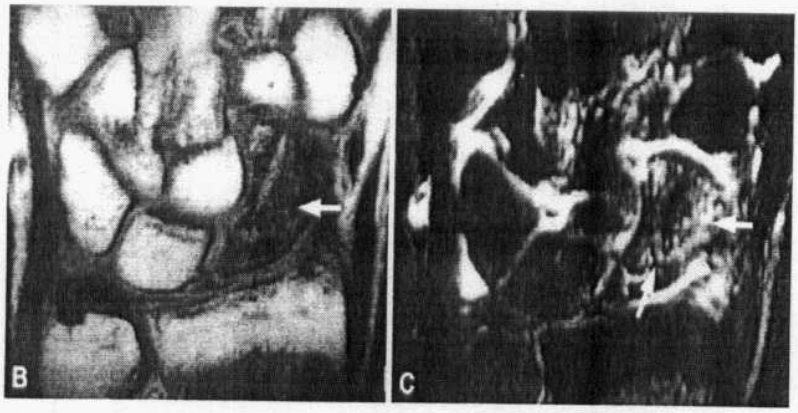

Fig.(60) (B) T1-weighted coronal image shows diffuse low signal intensity sclerosis (arrow). **(C)** short TI inversion recovery coronal image most accurately depicts hyperintense hyperemic marrow in the waist and distal pole of the scaphoid (arrow).(A discrete scaphoid fracture is not identified **(Quoted from McAlinden 2001).**

Intravenously administered galodlinium contrast produces enhancement of hyperemic tissue at the fracture site and adjacent subchondral bone marrow. This is assessed on T_1-weighted fat-suppressed images. Absence of proximal pole bone marrow enhancement indicates lack of vascular perfusion in the development of AVN. Fracture healing demonstrates hyperemia at the fractures site and adjacent marrow. Nonunion is characterized by persistent low signal intensity on T_1, T_2, and post-contrast fat-suppressed T_1-weighted images. High signal intensity fluid may be seen separating fracture fragments. Callus or fibrous union may also demonstrate low signal intensity on T_1- or T_2 weighted images ***(Rennie and Finlay, 2003).***

Kienbock's disease (KD)

Lunate bone is susceptible to a vascular necrosis. Loss of blood supply to the lunate has been attributed to fractures, repetitive trauma causing micro fractures and traumatic injury to the ligaments that carry blood supply to the lunate . kienbock's disease commonly affects males in the teens (**Fig. 61**) ***(Georges , et al., 2003).***

Fig.(61) Kienböck's disease. An anteroposterior radiograph displays sclerosis and collapse of the lunate (arrows) associated with negative ulnar variance**(Quoted from Stoller and Brody, 1997).**.

Lichman described radiographic staging criteria. ***stage I*** lunates are normal radiographically (**Fig. 62**), with ***stage II*** there is sclerosis or increased density without collapse (**Fig. 63**), ***stage III*** demonstrate collapse and fragmentation without or with fixed scaphoid rotation and scapholunate dissociation (**Fig. 64**), ***stage IV*** disease includes features of stage III with associated radiocarpal and mid carpal arthrosis ***(Brequist, 2003).***

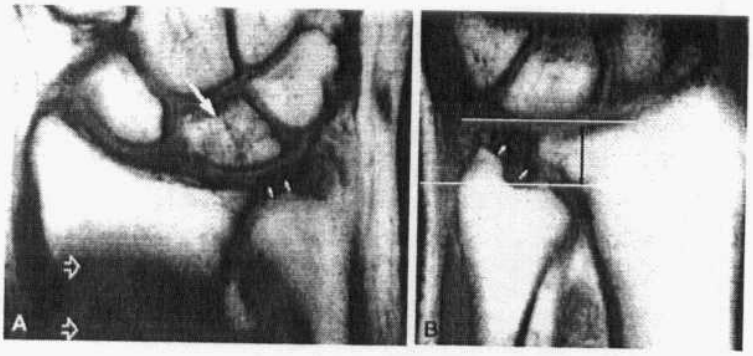

Fig.(62) (A) Recovering fatty marrow signal intensity (large arrow) is present after treatment of stage 1 Kienböck's disease of the right wrist. The lunate and triangular fibrocartilage (small arrows) is normal. A low signal intensity postoperative artifact secondary to radial shortening is present (open arrows). **(B)** The untreated left wrist shows severe negative ulnar variance (black double-headed arrow) and deformed but intact triangular fibrocartilage (white arrows). The lunate marrow is unaffected**(Quoted from Stoller and Brody, 1997).**

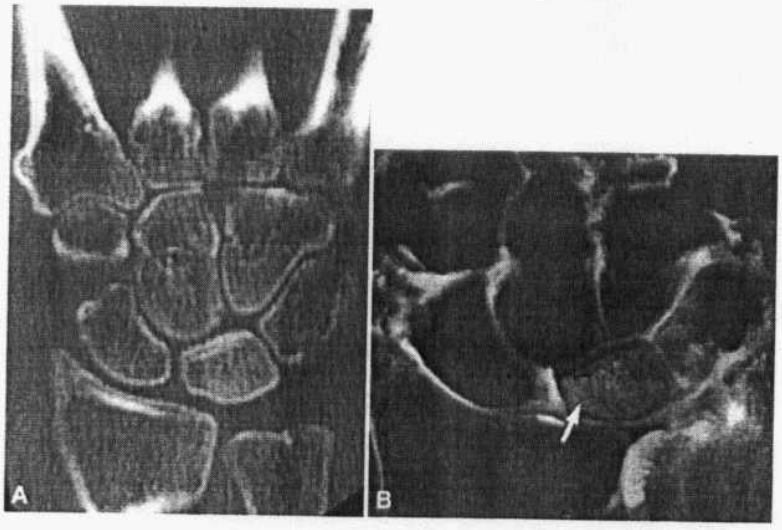

Fig.(63) Stage II Kienböck's disease with (A) increased lunate density (sclerosis) on coronal reformatted CT scan and (B) corresponding marrow hyperintensity on fast STIR coronal image**(Quoted from Stoller and Brody, 1997).**

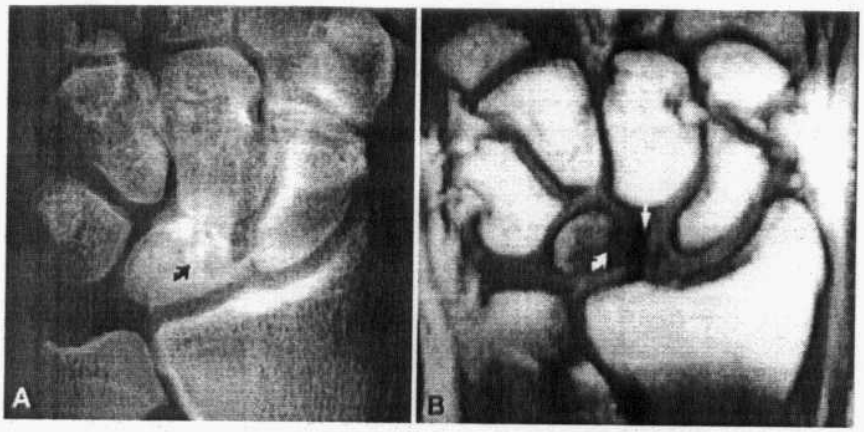

Fig.(64) (A) An anteroposterior radiograph shows lunate collapse (curved arrow) and proximal migration of the capitate in stage III Kienböck's disease. **(B)** A T1-weighted coronal image better depicts necrotic marrow (curved arrow) and lunate collapse in the radial border (straight arrow) **(Quoted from Stoller and Brody, 1997).**

Other lesions in the lunate that may simulate kienbocks disease include intraosseous ganglion cyst and marrow oedema or subchondral cyst formation that may occur from ulnolunate impaction, both of these intities are focal and have high signal intensity on T_2-WI. The diagnosis of kienbock's disease (KD) is certainly more definite when the entires bone is involved or when there is low signal intensity on both T_1- W & T_2- W images, but must be considered in the defferential for focal lesions that are high signal intensity on T_2 -W images as well ***(Kaplan et al., 2001).***

The vascular supply to the capitate is similar to that of the scaphoid placing the proximal third at risk after fractures.

A vascular necrosis of the other carpal bones (**Fig. 65**) is rare due to their rich vascular supply. Osteonecrosis of all carpal bones (Caffey's disease) is rare ***(Brequist, 2003).***

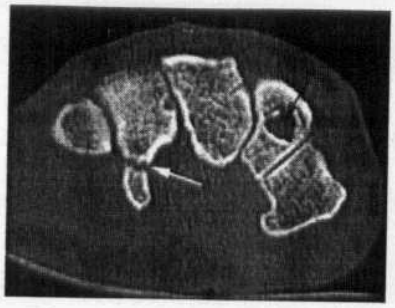

Fig.(65) Axial CT scan demonstrating a fracture of the hook of the hamate (white arrow) that was not seen on plain radiography. An incidental intraosseous ganglion (black arrow) is present**(Quoted from McAlinden, 2001).**

Routine radiographs are useful for evaluating ulnar length,, normally the ulna should be the same length as the radius at their articular junction, when the ulnar length in increased (ulnar positive variance)(**Fig. 66)** one should consider ulnar lunate impaction syndrome. Which may cause focal cystic change in the adjacent lunate this should not be confused with a vascular necrosis . the incidence of a vascular necrosis is increased in patients with ulnar shortening (ulnar minus variance)(**Fig. 67)** greater than 2mm. the neutral posteroanterior radiograph is used to measure ulnar length ***(Brequist, 2003).***

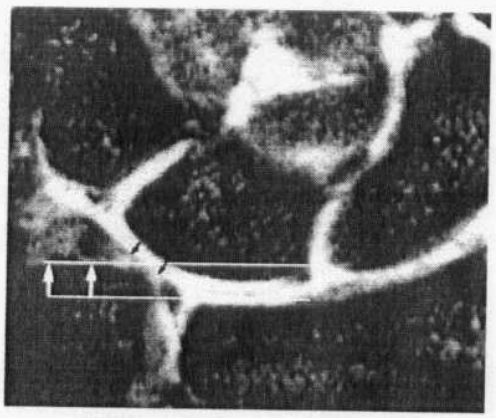

FIG.(66) Positive ulnar variance (white arrows), triangular fibrocartilage perforations (black arrows), and a torn lunotriquetral ligament are features of ulnolunate (ie, ulnocarpal) abutment syndrome **(Quoted from Stark and Bradly, 1999).**

Fig.(67) Negative ulnar variance with the articular surface of the ulna projecting proximal to the articular surface of the radius (arrow) **(Quoted from Stark and Bradly, 1999).**

Synovial lesion

Pigmented villo nodular synovitis (PVNS):

Pigmented villo nodular synovitis (PVNS) is a monoarticular synovial proliferative disorder that typically affects large joints in adult (30 to 50 years of age). The knee is most commonly affected, patients present with swelling and pain in the involved joint.

The wrist is not commonly involved, MR features are characteristic and present more specific diagnosis of PVNS than other arthropathies.

Hemosiderin deposition and fibrosis in proliferating synovial tissue result in area of low signal intensity on both T_1& T_2-W images, patients frequently develop recurrence (50%) following synovectemy therefor MRI is also important for follow up in patients treated from PVNS (**Fig. 68**) ***(Brequist, 2003).***

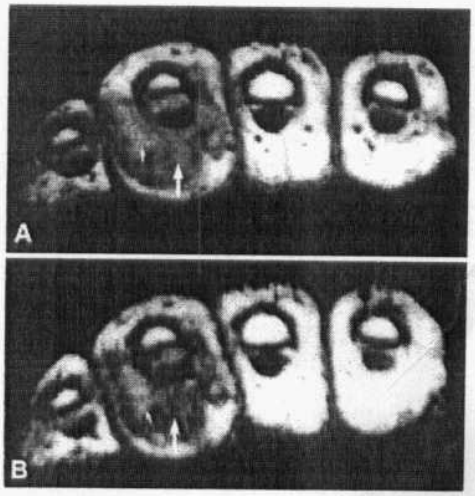

Fig..(68) (A) giant cell tumor of the tendon sheath (ie, extraarticular pigmented villonodular synovitis; large arrows) demonstrates low signal intensity on axial (A) intermediate-weighted and **(B)** T2-weighted images. Minimal fluid signal intensity (short arrows) is seen **(Quoted from Stoller and Brody, 1997).**

Synovial chondromatosis:-

The condition is the result of cartilaginous, osteoid or oseto_ cartilaginous metaplasia of synovium, males outnumber females 2 : 1, the condition is monoarticular. The distal radioulnar joint is commonly involved.

There arephases of this progressive process. The first phase is intrasynovial proliferation, phase 2 is active synovial disease with loose bodies, and phase 3 is inactive synovial disease with loose bodies ***(Roulot and Lebviet , 1999).***

Patients present with progressive swelling, pain and decreased range of motion of involved joint. routine radiographs demonstrate soft tissue swelling, multiple dense shadows (millimeters to centimeters in size) bone erosion and varying degrees of calcification or ossification in or about the joints or along the tendon sheaths of the hand and wrist ***(Resink, 1996).***

On MRI there are joint effusion, hypertrophic synovium and in late stage, low signal intraarticular bodies ***(Kramer, 1993).***

Synovial cyst:

Small amount of fluid in the pisotriquentral synovial recess normally may be seen, but when it becomes large in amount it may be a possible source of pain.

MRI appearance of pisotriquentral synovial cyst is that of a rounded or elongated mass on the volar aspect of the wrist, just proximal to the

pisiform, that is low signal intensity on T_1_W images and high signal on T_2 _W image (**Fig. 69**) . When it measures one cm. or more in diameter, we mention it as a synovial cyst that may be a pain source ***(Kaplan et al., 2001).***

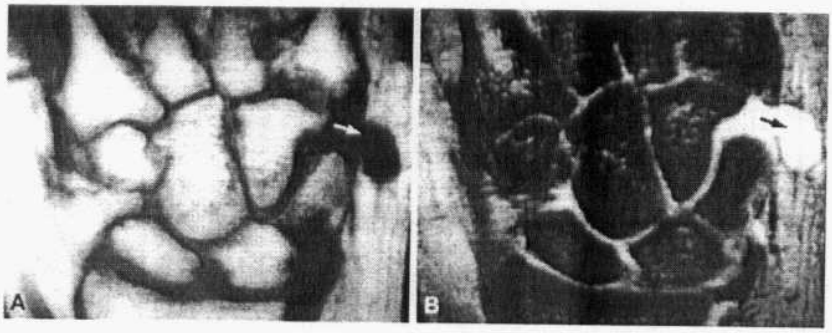

Fig.(69) Synovial cyst (arrows) communicates with the hamate triquetral joint. The lesion demonstrates **(A)** low signal intensity on a T1-weighted coronal image and **(B)** hyperintensity on a T2*-weighted coronal image **(Quoted from Stoller and Brody, 1997).**

Masses of the wrist

Bengin tumors and tumor like condition in the hand and wrist occur much more frequently than malignant neoplasms ***(Berquist , 2003).***

Bengin osseous lesions:

_ Benign tumor s of hand and wrist.

BENIGN LESION	*PERCENTAGE*
Enchondroma	54 %
Gaint cell tumor	5 %
Osteoid osteoma	6 %
Aneurysmal bone cyst	6 %
Osteochondroma	4 %
Osteoblastoma	4 %
Chondomyxoid fibroma	4 %
Exostosis	3 %
Intraosseous ganglion	8.5 %
Simple bone cyst	1.2 %
chondoblastoma	0.3 %

(Berquist, 2003).

Enchondroma:

Enchondrmas are the most common benign bone tumour in the hand and wrist ***(Girgis, et al., 2000).***

Enchondromas are composed of lobules of hyaline cartilage and they are usually centrally located in the mataphysis, when symptoms develop without fracture malignant degeneration should be considered ***(Berquist, 2003).***

Radiographically, enchondromas present as well defined lucent lesions with area of matrix calcification in some cases cortical expansion and thickening may be evident (**Fig. 70**).

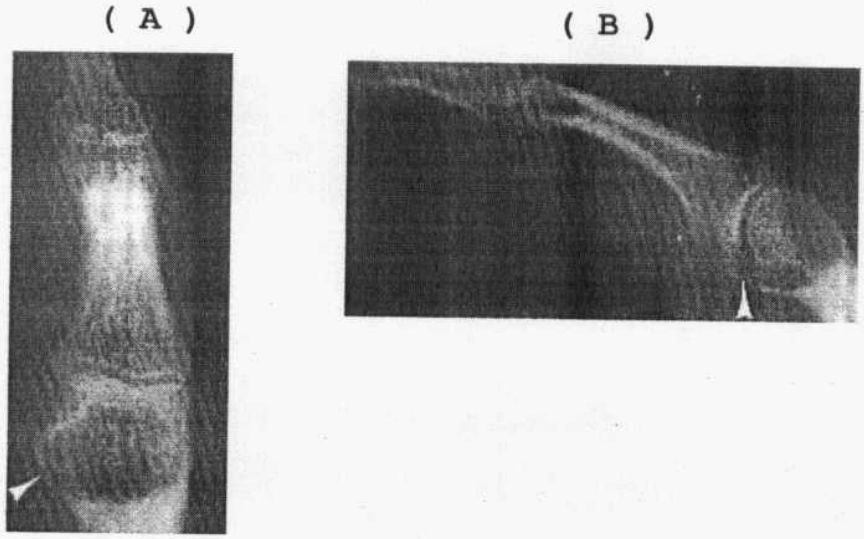

Fig.(70) Posteroanterior **(A)** and lateral **(B)** radiographs of an enchondroma in the distal aspect of the proximal phalanx there is pathological fracture (arrow head) that resultedin its detection **(Quoted from Berquist, 2003).**

MRI features show lobular high signal intensity on T_2 _W images, this was felt to be related to higher water content of hyaline cartilage, the signal intensity on T1 _W images is isointense in comparison with muscle. Differentiation of benign from malignant is not consistent on MR images, cortical destruction and soft tissue involvement are useful features ***(Brequist, 2003).***

Giant cell tumors:

Giant cell tumors are locally aggressive lesions representing about 5% of benign bone tumors, the lesions are most common after age of 20 (20 to 40 years), the lesions is more common in females than males ***(Campanacci, 1999).***

Radiographs demonstrate alytic lesion in the metaphysis extending to subchondral bone, the margins may be well or poorly defined, cortical expansion, thinning and fracture are evident in 33% to 50% of cases.

On MRI (**Fig. 71**)the lesion has signal intensity similar to that of muscle on T_1_ W images, signal intensity is inhomogenous on T_2 _W images with areas of high signal intensity, intermediate intensity and low intensity due to hemosiderin in 63% of cases ***(Berquist, 2003).***

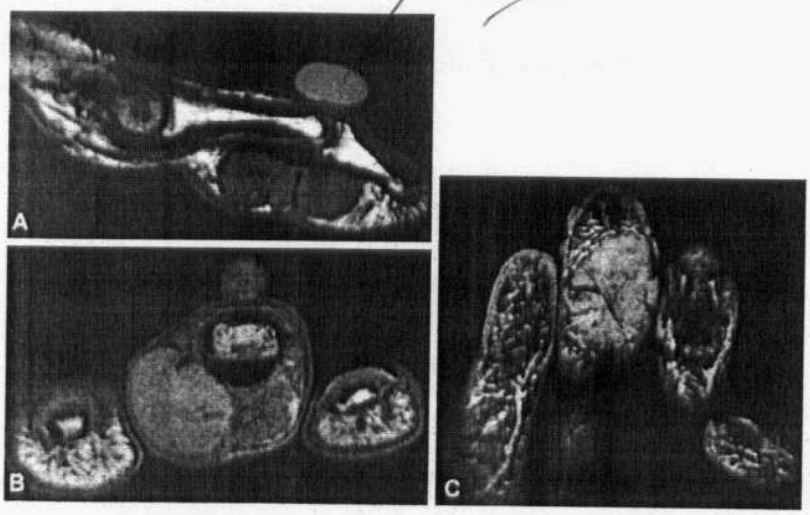

Fig.(71) Giant cell tumor of the flexor tendon sheath is low to intermediate in signal intensity on T1-weighted sagittal **(A)** and axial **(B)** images. On volar T2*-weighted coronal images through the phalanges, however, it demonstrates intermediate intensity. On T2*-weighted sequences due to the effect of hemosiderin**(Quoted from Stoller and Brody, 1997).**

Osteoid osteoma (Fig. 72):

Osteoid osteomas are common benign bone lesions accounting for 6% of benign bone tumors, though osteoid osteomas can occur at any skeleton location, about 50% involve the femur and tibia. most are cortical and diaphyseal or metaphyseal.

Osteoid osteomas can occur in elderly but most are reported in patients between 10 and 20 years of age, lesions are much more common in males than females, the classic presenting complaint is pain at night *(Broquist, 2003).*

MR appearance :

MR appearance of osteoid osteomas has become more clearly described in recent years on T_1_WI, the nidus is low signal intensity with low intensity osseous edema, the nidus may be high signal intensity on T_2_ WI with surrounding marrow edema and synovial or soft tissue inflammation. When there is significant calcification in the nidus, the signal intensity may be low on T_2. WI ***(Brequist, 2003).***

Fig.(72) Osteoid osteoma .Tomogram of the wrist demonestrates a sclerotic focus in the wrist (arrow) **(Quoted from Berquist, 2003).**

Aneurysmal bone cyst (Fig. 73):

Aneurysmal bone cysts are most commonly seen in patients 5-20 years of age. More than 50% of lesions occur in the long bones and up to 30% involve the spine. 6% involve the hand and wrist ***(Coumpancci M, 1999).***

Aneurysmal bone cysts are blood filled structures with cavernous spaces separated by fibroblasts and osteoid bone. Radiographs typically demonstrate an eccentric lytic lesion with thinning of cartex and bony expansion. Septations or trabeculated appearance is common.

MRI can demonstrates a well-defined, lobulated lesion with septations and multiple fluid- levels ***(Brequist, 2003).***

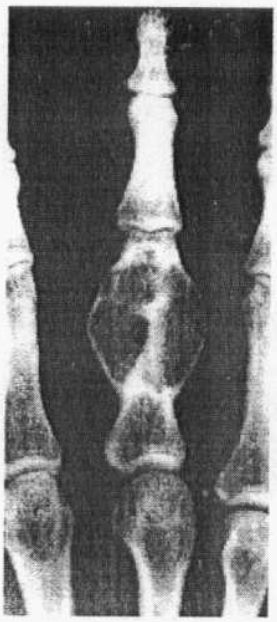

Fig.(73) Aneurysmal bone cyst . Posteroanterior radigraph of the middle finger demonestrates a lytic expanding lesion of the proximal phalanx **(Quoted from Berquist, 2003).**

Malignant osseous lesions:

Primary and secondary osseous neoplasms in the hand and wrist are uncommon to rare depending on the histology ***(Caute et al., 1998).***

3% of malignant fibrous histiocytomas and 2% of chondrosarcomas involve the hand and wrist Osteosarcomas and Ewing's sarcoma are reported but rare in the hand and wrist ***(Saitoh, et al., 2000).***

MR image features have not been useful for histologic differentiation of malignant bone lesions therefore staging for marrow or cortical bone involvement and soft tissue extension is the primary indication for MRI of suspected malignant osseous lesions ***(Berquist, 2003).***

Soft tissue masses:

Soft tissue masses in the hand and wrist are not uncommon. The majority are benign ***(Weiss, et al., 2001).***

Ganglion cysts:

Ganglion cysts are the most common soft tissue mass on the hand and wrist. Synovial herniation, tissue degeneration and repetitive trauma have been suggested as possible etiologic factors. The lesions most often occur over the dorsum of wrist ***(Berquist, 2003).***

Associated tears in TFCC are associated with ulnar ganglia. Radial ganglia may be associated with ligament tears or degeneration. Ganglions may be cystic, filled with mucoid material or complicated by haemorrhage.

Radiographs may reveal a focal soft tissue prominence or dorsal erosion at the lunate, ultrasound demonstrates a cystic lesion. MRI demonstrates well defined lesion with high intensity on T_2 and low intensity on T_1 weighted images(**Fig. 74**) ***(Borquist, 2003).***

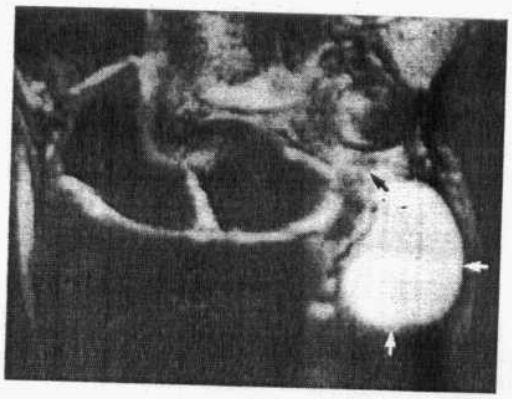

Fig.(74) A large ganglion cyst (white arrows) projects from the ulnar aspect of a torn triangular fibrocartilage (black arrow) **(Quoted from Stoller and Brody, 1997).**

Lipomas:

Lipomas account for 5% of benign tumours in the hand and wrist ***(Goodman, et al., 1997).***

Lipomas may be superficial (subcutaneous) or deep. The former are difficult to separate from subcutaneous fat except in the hand and wrist where there is less subcutaneous fat compared with the trunk or proximal extremities, most lesions are solitary though multiple lesions are reported in

5% to 7%, on MR images (**Fig. 75)** the mass has fat signal intensity on T_1 and T_2_ WI ***(Berquist, 2003).***

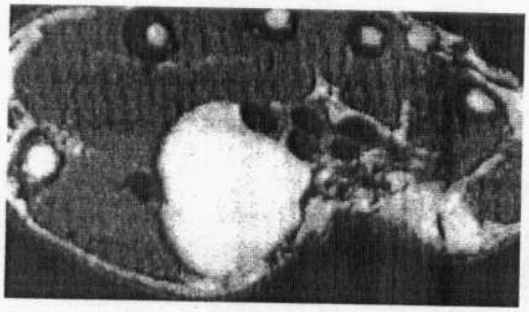

FIG.(75) Axial T1_WI of well defined, slightly septated lipoma **(Quoted from Berquist, 2003).**

Glomus tumours:

Glomus bodies are arteriovenous anastomoses responsible for thermo_ regulation, the unit consists of an afferent arteriole, tortuous, arteriovenous anastomoses collecting viens and a neurovascular system that regulates flow through the anastomoses. glomus bodies are present in the dermis throughout the body but they are most evident in the digits of the hand and foot ***(Theumann, et al., 2002).***

These lesions occount for only 1.2% to 5% of all hand tumours, lesions may be painful, often exacerbated by changes in temperatures, lesions are usually solitary but multiple tumour are reported in 2.3%. Radiographs demonstrate smooth bone erosion adjacent to the lesion in 22% to 60% of cases.

MR images demonsertrate well defined, intermediate or low intensity on T_1. WI and homogenous high intensity on T_2. WI and STIR

images, lesion enhance uniformly after gadolinium injection ***(Berquist, 2003).***

Malignant soft tissue tumours:

Malignant soft tissue tumors in the hand and wrist are uncommon, malignant fibrous histocytoma is the most common malignant soft tissue tumor in older adults (older than 45 years) other malignant lesions involving the hand and wrist include synovial sarcoma, fibrosarcoma, malignant peripheral nerve sheath tumours, epitheloid sarcoma and extra-skeletal chondrosarcoma ***(Weiss and Goldblum, 2001).***

The MRI feature of malignant soft tissue masses are not specific. Lesions are typically poorly marginated with low signal intensity on T_1-WI & inhomogenous high signal intensity on T2-WI. The lesions show irregular enhancement after intravenous gadolinium. Necrotic areas don't enhance ***(Berquist, 2003).***

Summary

&

Conclusion

SUMMARY AND CONCLUSION

The wrist is a complex joint. Because of its great mobility and functions, it is one of the commonly injuried joint in the human body. Diagnosis of wrist lesions should be achieved to prevent long-term disability.

Magnetic resonance imaging is an effective modality to determine the wrist lesions as it demonstrates soft tissue, muscles, nerves and blood vessels.

It can also demonstrate erosions and cartilage thinning than plain radiograph. and MRI can directly visualize and monitor changes in synovium and bone that precede actual bone erosion.

MRI is an accurate and effective method for the non- invasive evaluation of pain in the wrist. It allows earlier detection of an abnormality in the triangular fibrocartilage complex (TFCC), cartilage, or bone marrow of carpal bones and is helpful in formulating the extensive differential diagnosis in patients with ulnar wrist pain and limitation of motion.

About 16% of scaphoid fractures are not evident on the initial radiographs, and MRI is an excellent method for detecting these lesions. MRI is the investigation of choice in avascualr necrosis and has an increasing role in internal derangement, trauma and soft tissue lesions. It has been reported to be as sensitive as bone scintigraphy in the detection of AVN and even more specific.

MRI provides an excellent modality for visualizing the full spectrum of the abnormalities of the ulnolunate abutment syndrome. It can also demonstrate subchondral cystic changes and subchondral sclerosis in the lunate.

Tears of the wrist ligaments are common causes of chronic wrist pain and instability. Although arthrography is quite accurate for the identification of tears of the intercarpal ligaments, MRI is noninvasive and can detect other causes of wrist pain.

MRI can demonstrate the fractures, Contusion, Physeal injury or focal bridge formation.

Athorough understanding of the osseous and soft tissue components of congenital malformations is of critical importance to the implementation of appropriate therapy. MRI is valuable for defining both soft tissue and bony anatomy in cases of complex congenital malformations.

conclusion

MR imaging is an effective modality for determining the wrist lesions as it demonstrates a broad spectrum of abnormalities including those of bony, cartilaginous, ligamentus origin. Imaging of the wrist should always begin with plain film examination. MR imaging is the only imaging technique that can directly depict the interosseous ligaments and the TFCC. It is the imaging technique of choice for early diagnosis of avascular necrosis, for tumor staging and for evaluating soft tissue masses.

MR imaging enables non invasive global examination of he wrist that is extremely sensitive in detecting osseous and soft diseases.

References

Anderson MW, Kaplan PA, Dussault RG et al., (1998): Magnetic resonance imaging of the wrist. Curr Probl Diagn Radol, Nov/Dec: 189-226.

Back L ,BakS. Gaster p et al.,(1997): MR imaging of the wrist in carpal tunnel syndrome. Acta Radiologica;38(6):10p50-52

Berger RA (1998): General anatomy in: Cooney WP III Linsheid, RL, Dobyns JH, eds. The wrist diagnosis and operative treatment. St. Louis: Mosby, 32-60.

Berquist (2003): MRI of Muscloskетelal system, 4th ed. Philadelphia; Lippincott Williams & Wilkins, 772-841.

Bogumill G (1998): Anatomy of the wrist, Philadelphia, PA : WB Saunders, 14-19.

Brown RR, Flizar E, Cotton A, et al., (1998): Extrinsic and pathologic anatomy at MR arthrography with three compartment enhancement. Radiographics, 18: 667-674.

Buchberger W (1997): Radiologic imaging of the carpal tunnel. Eur J Radiol; 25: 112-1

Bruckner and K. Khan (2005): Clinical sports medicine 2nd ed. Chapter 16.

Carcic-Elias M and Dobynd JH (1998): Bone and /Joints in: Cooney WP III linscheid RL, dobyns JH. The wrist: diagnosis and operative treatment. ST. Louis: Mosby, 61-72.

Campanacci M (1999): Bone and soft tissue tumours New York: springer Verlag.

Catherine W(1999): Hand book of MRI technique,2nd ed.Pa:Blackwell;312 -319.

Caute TG, Steiner GC, Beltran J, et al., (1998): Chondrosarcoma of the short tubular bones of the hands and feet. Skel Radiol, 27: 625-632.

Cerezal L, Pinal Abascal F et al., (2002): Imaging finding in ulnar sided wrist impaction syndromes, radiographics; 22 (1): 105-21.

Chein AL, Jacobson Ja, Martel W et al., (2001): Focal radial styloid abnormality ad a manifestation of de quarvian teno synovitis. AJR; 177: **1383-1386.**

Cimmino MA, Innocenti S, LIVRONE Fet al.,(2003): Dynamic gadolinium- enhanced Magnetic resonance imaging of the wrist in patients with rheumatoid arthritis can discriminate activ from inactive disease. Arthritis Rheum; 48(5):1207-13.

Edeiken J, Depalma AF, Hodes PJ (1996): Osteoid osteoma (roentgenographic emphasis) Clin Orthop; 49: 201-206.

Georges Y, John Haller, James Olsen et al., (2003): Essential of Musculo skeletal imaging, 554-563.

Girgis WS Epstein RE (2000): Magnetic resonance imaging of the hand and wrist, semin Roentgenol; 35: 286-296.

Gobby JL, Dixon AK, Beatcroft PWP, et al., (2001): MR imaging of the wrist: effect on clinical diagnosis and patient care. Radiology; 220: 589-593.

Goodman HJB, Richards AM, Klassen MF (1997): Use of magnetic resonance imaging on a large lipoma of the hand. A case report. Aust NZJ Surg; 67: 489-491.

Gray H (1987): Gray's anatomy: Crown publishers,.

Haims AH, Schweitger ME Marroison wB, et al., (2003): Limitation of MR imaging in the diagnosis of peripheral tears of triangular fibrocartilage of the wrist. AJR; 178: 419-422.

Han B, Jang S, Chang Y,et al.,(2003): kinematic MRI of the wrist ,AM J Phys Med Rehabil; 82(1):17-20.

Herneth A, Seigmeth A, Bader T et al., (2001): Scaphoid fractures: evaluation with high spacial resolution US initial results. Radiology; 220: 231-35.

Hobby JL, Dixon AK, Bearcroft PWP,et al.,(2001):MR imaging of the wrist:effect on clinical diagnosisand patient care.Radilogy;220:589-593.

Huang HW and Strauch RJ (2000): Pollicis longus tenosynovitis: a case report and review of the literature J Hand Surg; 25A: 577-579.

Ikeda M and Oka Y (2000): Cystic lesion in the carpal bone Hand Surg; 5: 25-32.

Kaplan P, Helms C, Dussautt R et al., (2001): Musculoskeletal MRI, Ist ed., WB saunders company; 347-374.

Keogh C , Wong A , Wells N et al., (2004): High resolution sonography of the triangular fibrocartilage: Initial experince and correleation with MRI and arthropathy. AJR;182: 333-36.

Kramer J (1993): MR appearance of idiophatic synovial osteochondromatosis. J Comput Assist Tomogr; 17: 722: 776.

McAlinden P S (2001): Imaging of the wrist. Radiology; 216: 144-151.

Mesgrzadeh M, Schneclk CD, Bonakdarpour A et al., (1996): Carpal tunnel: MR imaging part (II) carpal tunnel syndrome, clin radial., 53 (2): 749-54.

Metz V, Wunderbaldinger P and Gilula L (1996) : Update of imaging techniques of the wrist and hand. Clinical Plastic surgery; (3) :369-74. (3) :369-74.

Monallge K, Dai G, Chu A, et al., (1999): Quantitative MR imaging of carpal tunnel syndrome. AJR, 17: 1581-86.

Murphey D. Mark, John F, Carroll, et al.,(2004): Benign Musculoskeletal Lipomatous Lesions. RadioGraphics 2004; 24: 1433-1466.

Nadja Saupe, Klaas P. Prüssmann, Roger Luechinger, et al., (2005): MR Imaging of the Wrist: Comparison between 1.5- and 3-T MR Imaging—Preliminary Experience Radiology 2005 234: 256-264.

Partik B, Rand T, Protter Klieber M et al., (2002): Patterns f Gd enhanced MRI of Radiocarpal joints of healthly subjects, AJR, 179: 193-97.

Potter HG, Asnis-Ernberg L, Weiland AJ et al.,(1997): the utility of hig resolution Magnetic resonance imaging in the evaluation of the triangular fibrocartilage complex of the wrist, J Bone Joint Surg Am ;79(11):1675-84.

Rennie W and Finaly D (2003): Post traumatic Cyst like defects of the scaphoid late sign of occult microfracture and useful indicator of delayed union. ARJ; 180: 1655-58.

Resnick D (1996): Bone and joint imaging, 2nd ed. Philadelphia: WB Saunders.

Rosse C and Rosse PC (1997): Hollingsheads textbook anatomy. Philadeliphia: Lippincott-Reaven Publichers,: 239-309.

Roulot E and Lebviet D (1999): Primary osteoschonolromatosis of the hand and wrist. A report of a series of 21 cases and literature review. Rev. Rheum; 66: 296-266.

Saitoh S, Hatori, M, Ehara S (2000): Ewing\s sacrcoma of the middle finger in an infant; 23: 379380.

Sakai, K, Tsutsui T, Aoi M, et al., (2000): Ulnar neuropathy caused by alipoma in Guyon's canal Med Chir, 40: 335-338.

Schimmel-Metz, Metz VM, Totterman SMS, et al.,(1999): Radiologic measurement of the scapholunate joint:implications of biologic variation in scapholunate joint morphology.J Hand Surg 24A:1237-1244.

Schreibman K, Freeland A, Giluta L et al.,(1997): Imaging oof the hand wrist, orthopedic clinics of north America; 28(4): 537-82.

Scott P, Robert E and Murray K (1997): MR imaging of the wrist, Radiology chinics of North America; 34(1): 145-61.

Seymour R and white P (1998): Magnetic resonance imaging of painful wrist BRJ Radiol;71(852):1323-30.

Siegel S, White L and Brahme S (1996): Magnetic resonance imaging of the musculoskeletal system. Part 5. the wrist, Clin ortho; (332):281-300.

Skeogh C, Wong A, Wells N et al., (2004): High resolution songongraphy of triangular fibrocartilage: initial experience and correlation with MRI and Arthrography. AJR; 182: 333-336.

Smith D (1995): MR imaging of normal and injuried wrist ligaments. MRI clinics of North America; 3 (2): 229-48.

Stark D & Bradly W (1999): Magnetic resonance imaging, 3rd ed., Pa: Mosby; 1226-94.

Steinborn M, Scuurmann M, Staebler A et al., (2003): MR imaging of ulno carpal impaction after fracture of distal radius; AJR; 181: 195-8.

Stoller D and Brody G (1997): MRI in arthopedics and sports medicine, 2nd ed, pa: Philadeliphia, lippincott William & Wilkins: 851-984.

Swen WAAA, Jacobs JWG, Hubach PCG, et al., (2000): Comparison of songography and magnetic resonance imaging for the diagnosis of partial tears of finger extensor endons in rheumatoid arthritis. Rheumatology; 39: 55-62.

Theuman NH, Goettmann S, Leviet D et al. (2002): Recurrent glomus tumours of finger tips, MR: imaging evaluation. Radiology; 223: 14-151.

Timins M, Connel S, Erickson S et al., (1996): MR imaging of the wrist: normal finding, that may simulate disease. Radio graphics; 16: 987-95.

Totterman S, Miller R, Wasserman B et al., (1993): intrinsic and extrinsic carpal ligaments evaluation by three dimensional MR imaging AJR; 160: 117-23.

Totterman SMS, Miller K (1996): Scapholunate ligament: normal MR appearance on three dimensional gradient recalled echo images. Radiology; 200: 237241.

Viegas SF, Crossley M, Marzke M et al. (1991): The fourth carpometa carpal joint. J Hand Surg; 16A: 525-533.

Weiss SW, Goldblum JR (2001): Enzinger and weiss' soft tissue tumours, 4th ed. St Louis: Mosby.

المخلـص العربي

يعد مفصل الرسغ من المفاصل المركبة وهو من أكثر المفاصل الجسم تعرضاً للإصابة وذلك لكثرة حركته ووظائفه. والتشخيص الدقيق لآفات الرسغ تعتبر شديدة الصعوبة، والوصول إلى التشخيص الدقيق لآفات الرسغ هام لمنع طول فترة العجز وإعادة الوظائف الهامة لهذا المفصل المركب.

يتم التعرف على الوصف التشريحي لمفصل الرسغ من خلال الأشعة السينية، والأشعة المقطعية ، تصوير المفاصل بالصبغة ، المسح الذرى للعظام، والأشعة المقطعية باستخدام الكمبيوتر، أما فحص الرنين المغناطيسي فقد أمدنا بمعرفة الوصف التشريحي الدقيق لهذا المفصل المركب ومعرفة الآفات المختلفة التي تصيبه والتي من الصعب رؤيتها بالأشعات المختلفة الأخرى حيث يعتبر هو الفحص الأمثل في العديد من الآفات مثل التنخر اللاوعائى لعظام اليد وأورام الأنسجة الرخوة.

كما يساعد فحص الرنين المغناطيسى على التشخيص الدقيق لتمزق الأربطة والمثلث الغضروفى الليفى المركب.

دور التصوير بالرنين المغناطيسى فى تقييم آلام مفصل الرسغ

(مقـــال)

مقـــدم مـــن

الطبيب / أحمد سعد الدين على معالى
بكالوريوس الطب و الجراحة

توطئة للحصول على درجة الماجستير فى الأشعة التشخيصية

المشرفون

الأستاذ الدكتور
مصطفى سنبل
أستاذ الأشعة التشخيصية
كلية الطب جامعة الأزهر

الأستاذ الدكتور
إسماعيل أحمد حمودة
أستاذ العظام
كلية الطب جامعة الأزهر

الأستاذ الدكتور
حسين عبد العزيز
أستاذ مساعد الأشعة التشخيصية
كلية الطب جامعة الأزهر

جامعة الأزهر
كلية الطب 2006